Ecological Indicators 115 (2020) 106392

Contents lists available at ScienceDirect

Ecological Indicators

journal homepage: www.elsevier.com/locate/ecolind

Climate change weakens the positive effect of human activities on karst vegetation productivity restoration in southern China

Luhua Wu[a,b,c], Shijie Wang[a,c], Xiaoyong Bai[a,d,e,*], Yichao Tian[f], Guangjie Luo[e], Jinfeng Wang[a,g], Qin Li[a,c], Fei Chen[a,g], Yuanhong Deng[a,c], Yujie Yang[a,c], Zeyin Hu[a,c]

[a] State Key Laboratory of Environmental Geochemistry, Institute of Geochemistry, Chinese Academy of Sciences, Guiyang 550081, China
[b] University of Chinese Academy of Sciences, Beijing 100049, China
[c] Puding Karst Ecosystem Observation and Research Station, Chinese Academy of Sciences, Puding 562100, China
[d] CAS Center for Excellence in Quaternary Science and Global Change, Xi'an 710061, China
[e] Guizhou Provincial Key Laboratory of Geographic State Monitoring of Watershed, Guizhou Education University, Guiyang 550018, China
[f] School of Resources and Environment, Qinzhou University, Qinzhou, Guangxi 535099, China
[g] College of Resources and Environmental Engineering, Guizhou University, Guiyang 550025, China

ARTICLE INFO

Keywords:
Karst
Climate change
Human activity
NPP
Contribution

ABSTRACT

China has conducted large-scale eco-afforestation projects in karst areas for mitigating rocky desertification in recent decades. However, the benefits of karst vegetation productivity restoration and the contributions of influencing factors are unclear. We analyzed the impacts of climate change (CC) and human activity (HA) on vegetation productivity change based on the net primary productivity (NPP) by using the partial derivatives and designing eight different scenarios. Results demonstrated that the average NPP over the entire vegetation-covered karst area exhibited an unremarkable increasing trend (0.92 g C m^{-2} yr^{-1}) and a major decline in NPP was detected in the areas where NDVI increased from 2000 to 2015 (0.44 million km^2, 29.07%). Solar radiation (−0.91 g C m^{-2} yr^{-1}) was the preponderant climatic factors exhibiting negative contribution to NPP changes. A significant positive contribution was caused by HA (1.53 g C m^{-2} yr^{-1}) on NPP variations, while a negative contribution was induced by CC (−0.61 g C m^{-2} yr^{-1}). CC and HA showed the more similar contribution proportion to NPP increasing (51.94% vs 48.06%), but with great difference (68.43% vs 31.57%) for NPP decreasing. 39.83% of the areas involved in NPP decreasing was attributed to the accelerating consumption of autotrophic respiration while the rest (60.17%) was contributed by rapid decrease of gross primary productivity, respectively. In southern karst area, HA showed a positive impact (59.07%) on NPP increasing. However, the negative contribution from CC (70.72%) due to the rapid and constant decline of solar radiation completely counteracted this, leading to a greater NPP decrease. This study stresses the importance of negative effect from CC on karst vegetation productivity change and provides location guidance for further implementation of ecological protection projects in southern China.

1. Introduction

As an important part of global vegetation, karst vegetation not only provides great carbon sink function, but also provides a series of ecological services, which has been the research focus in the field of global change. Net primary production (NPP), as a key parameter of terrestrial ecological process, reflects the vegetation productivity under natural circumstances (Zhao and Running, 2010; Hasenauer et al., 2012; Peng et al., 2017; He et al., 2018). NPP is widely used to estimate the supporting capacity of the earth and evaluate the sustainable development of terrestrial ecosystems (Gollnow and Lakes, 2014; Wu et al., 2015; S. Zhou et al., 2017; W. Zhou et al., 2017; Zhou et al., 2014). Moreover, it is also an important component and key link of global carbon cycle and gives significant effect on global carbon balance (Ben et al., 2018; Gahlot et al., 2017; Li et al., 2018b; Ogle, 2018; Pan et al., 2011; Piao et al., 2009; Tian et al., 2011; Yu et al., 2013).

Globally, karst rocks are abundant on the earth's surface and approximately 15.6% of land comprises karst areas (22 million km^2), where as much as 20% of the global population lives (Jiang et al., 2014). In China, the karst areas cover approximately 3.44 million km^2,

* Corresponding author at: State Key Laboratory of Environmental Geochemistry, Institute of Geochemistry, Chinese Academy of Sciences, 99 Lincheng West Road, Guiyang 550081, China.
E-mail address: baixiaoyong@vip.skleg.cn (X. Bai).

https://doi.org/10.1016/j.ecolind.2020.106392
Received 10 November 2019; Received in revised form 22 February 2020; Accepted 6 April 2020
Available online 15 April 2020
1470-160X/

accounting for more than one-third of its total land area. The karst area of southern China is one of the largest continuous karst areas worldwide, which covers 1.9 million km^2 and provides a variety of ecosystem services, such as water and soil conservation, climate control, and carbon sequestration (Chen et al., 2019b; Jiang et al., 2014; Tian et al., 2016). This area experienced serious rocky desertification driven by climate factors, population growth, and agricultural activities before about 2010, and was regarded as one of the most poverty-stricken areas in China, with a poverty population of more than 20 million (Zhang et al., 2017). To mitigate rocky desertification and relieve poverty, the ambitious afforestation and a large diversity of conservation projects were conducted there and a large area of farmlands and degraded lands were converted back to forests and grasslands (Brandt et al., 2017; Tong et al., 2018; Yang et al., 2019). After decades of efforts, China had become the country with the largest afforestation area, the highest conservation effort, and the fastest growth of forest covers in the world (Chen et al., 2019; Fensholt et al., 2012; Zhu et al., 2016). Afforestation and ecological engineering protections were particularly significant in karst area, which provided a great contribution to the greening of the earth and carbon accumulation (Brandt et al., 2018b; Chen et al., 2019a; Tong et al., 2018).

Climate change (CC) and human activity (HA) were the main factors affecting the change of vegetation productivity (Forkel et al., 2014; Huang et al., 2018; X. Liu et al., 2019; Y. Liu et al., 2019; Tong et al., 2020; Wang et al., 2016; Zeng et al., 2018). CC was more identified as a negative factor restricting the growth of vegetation productivity (Piao et al., 2015; Tong et al., 2018; Wen et al., 2018; Xu et al., 2019; S. Zhou et al., 2017; W. Zhou et al., 2017; Zhou et al., 2014; Zscheischler et al., 2014). Although previous studies demonstrated that several critical climatic constraints to plant growth were eased (Zhao and Running, 2010) and showed a strong promoting effect in middle-high latitudes of the Northern Hemisphere (Nemani et al., 2003), extensive studies found that CC was still an important factor restricting vegetation growth in some regions and its negative contribution even exceeded that of HA (Heinsch et al., 2006; Peng et al., 2017; Prestele et al., 2017; Bjorkman et al., 2018). It had been widely reported that recent climate-induced carbon losses had attracted widespread attention over the past decades in the large areas of Russia, Argentina and Peru (Peng et al., 2017), the Southern Hemisphere (Zhao and Running, 2010), Northern Hemisphere (Liu et al., 2015), Africa and other regions (Brandt et al., 2017, 2018a). Besides the influence of CC, HA was also an important factor affecting the growth of vegetation productivity. However, there were many controversies about the impact of HA on NPP increasing. In the past, many ecological projects had ignored the vegetation growth characteristics in karst area where plants grew on rocks, tended to absorb calcium and magnesium, and had a strong tolerance for drought, which resulted in low survival rate of afforestation and low recovery benefit (Zhang et al., 2017). This indicated that these positive human activities were difficult to have beneficial effects on vegetation restoration. By contrary, human interference was usually diagnosed as the main cause of land degradation and deforestation (Bai et al., 2013; Hansen et al 2013; Wu et al., 2017; Brandt et al., 2017). Although many studies suggested that although HA had provided a significant positive role in improving vegetation coverage and biomass increasing (Fang et al., 2014; Piao et al., 2015; Mao et al., 2016; Tong et al., 2017; Tong et al., 2020), the unobvious trend of annual NPP changes in most areas of China (79.9% of total vegetation covered areas of China) had raised some doubts about its positive effects (Li and Wang, 2018). This showed that vegetation productivity change was obviously uncertain in different regions under the combined influence of CC and HA due to different driving mechanisms. Furthermore, since the launch of the Grain to Green Program (GTGP) in 1999 (Tong et al., 2018; Delang and Yuan, 2015), the government had laid too much stress on how to speed up vegetation greening, but ignored its quality and benefits. Therefore, at present, it remained unclear where and at what scale such effects influenced on vegetation productivity and if vegetation productivity increased at a large spatial scale as expected, especially in rocky desertification mountainous areas where ecological projects were implemented intensively.

Here, this study aimed to separate effectively and assessed quantitatively the impact of CC and HA to the vegetation productivity evolution. We attempted to select NPP as an indicator to represent vegetation productivity and selected T (temperature), P (precipitation), and SR (solar radiation) as the evaluation indicators of main climatic factors. Then, the contributions caused by CC and HA to vegetation productivity were quantitatively evaluated by using the partial derivatives. Lastly, the contribution proportions of CC and HA to NPP increasing and decreasing were also evaluated by setting up eight different scenarios with consideration for the complexity of each driving mechanism and actual assessment needs. We had addressed the following scientific issues: (1) to investigate the change trend and spatial pattern of NDVI and NPP during 2000–2015; (2) to separate and quantify the impacts affected by CC and HA to NPP variations; and (3) to identify the critical control areas where CC and HA contributed to NPP increasing or decreasing. This study has significantly contributed to a better understanding of key influence factors contribution on vegetation productivity and shed lights on government policy-making and the reasonable layout of ecological restoration projects.

2. Study area

Karst landforms (buried, covered, and exposed carbonate rock areas) were widely distributed in China with a total area of 3.44 million km^2 (Jiang et al., 2014) (i.e., approximately 15.64% of global terrestrial karst area and 35.8% of China's total land area). In this study, the karst area (exposed karst area) was approximately 1.88 million km^2 (i.e., 19.58% of the total area of China) on the basis of statistics from spatial data (Fig. 1). However, the karst area covered by vegetation was only 1.51 million km^2, which accounted for 80.35% of the total karst areas (1.88 million km^2) in China. Regionally, it was divided into three major karst zones of southern China (0.82 million km^2), northern China (0.27 million km^2), and the Qinghai–Tibet Plateau (0.79 million km$^{2)}$, accounting for 43.62%, 14.36%, and 42.02% of the total karst area, respectively. Notably, a large concentrated contiguous karst area (0.54 million km^2) was located in the eight provinces (1.9 million km^2, including GZ (Guizhou), YN (Yunnan), CQ (Chongqing), HUN (Hunan), HUB (Hubei), GD (Guangdong), GX (Guangxi), and SC (Sichuan)) of southern China, accounting for 28.42% of the total areas of eight provinces. In this study, GZ, YN, HUN, HUB, GX, GD, CQ, SC, JX (Jiangxi), FJ (Fujian), ZJ (Zhejiang), JS (Jiangsu), AH (Anhui), HAN (Hainan), and TW (Taiwan) belonged to the southern provinces, QH (Qinhai) and TB (Tibet) belonged to the Qinghai-Tibet Plateau, and XJ (Xinjiang), GS (Gansu), NX (Ningxia), IM (Inner Mongolia), SAX (Shaanxi), SX (Shanxi), HN (Henan), HB (Hebei), SD (Shandong), BJ (Beijing), TJ (Tianjin), LL (Liaoning), JL (Jilin), and HLJ (Heilongjiang) belonged to the northern provinces.

3. Data

3.1. GPP and NPP dataset

The Gross Primary Productivity (GPP) and NPP data set on vegetated land at a 1 km resolution and an 8 day interval during 2000–2015 were obtained from MOD17A3, which was produced by the Numerical Terradynamic Simulation Group (NTSG) at the University of Montana (UMT) (http://www.ntsg.umt.edu/). The projection format was the equal longitude and latitude projection of WGS-84, and the ratio coefficient was 0.1. The annual NPP of terrestrial ecosystem was simulated by using the BIOME-BGC ecosystem process model. Since 2000, the MOD17A3 NPP data set was widely used in global and regional vegetation productivity and carbon cycle researches (Gonsamo et al., 2016; Guo et al., 2012; Haberl et al., 2007; Hasenauer et al.,

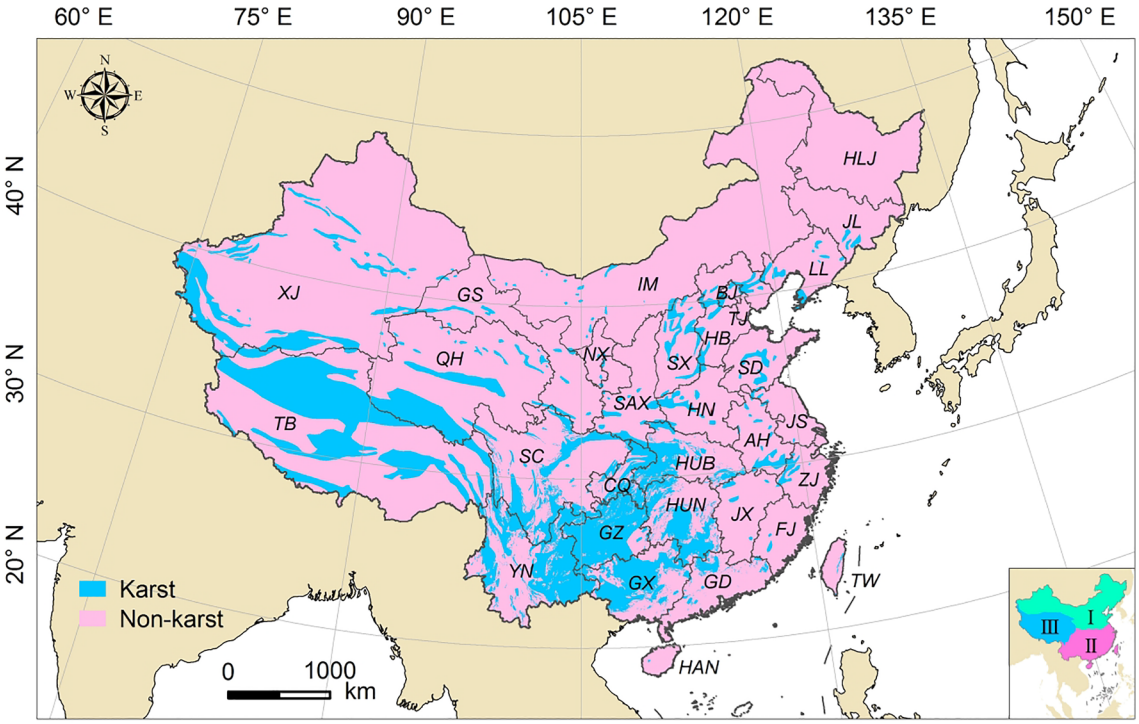

Fig. 1. Spatial distribution of karst area in China. I, II, and III in attached drawing in the lower right corner represents the northern China, the southern China, and the Qinghai-Tibet Plateau, respectively.

2012; He et al., 2018; Peng et al., 2017; Zhang et al., 2009). The NPP products had undergone four validation with the 3rd stage to improve the data quality (Morisette et al., 2002; Zhao et al., 2005; Heinsch et al., 2006; Nightingale et al., 2008; Hasenauer et al., 2012; Pan et al., 2014; Pan et al., 2015; Running et al., 2015). Uncertainty in the product was assessed and effectively quantified by annual NPP observations from flux sites and ancillary reference data (Running et al., 2015; Peng et al., 2017), and the data coincidence rate was over 91%. Based on these validations via multiple aspects from many researchers in the world, the MOD17A3 NPP product was suitable for use to evaluate vegetation productivity in karst area.

3.2. NDVI dataset

Vegetation index (NDVI, Normalized Difference Vegetation Index) could accurately reflect the vegetation cover on the surface. At present, the NDVI time series data, which was obtained from satellite remote sensing images based on SPOT/VEGETATION and MODIS, had been widely used in the monitoring of vegetation dynamic change, land use/cover change detection, macro-vegetation cover classification, and the estimation of net primary productivity. The annual vegetation index (NDVI) spatial distribution data set of China at 1 km resolution during 2000–2015 was the annual vegetation index data set since 1998. This data set was generated by the maximum synthesis method based on SPOT/VEGETATION NDVI satellite remote sensing data of continuous time series (Xu, 2018) and obtained from the Resource and Environment Data Cloud Platform of Chinese Academy of Sciences (http://www.resdc.cn/). This data set could effectively reflected the distribution and change of vegetation cover in different regions of China on temporal and spatial scales. It was of great significance for monitoring vegetation change, rational utilization of vegetation resources and other related fields of ecological environment.

3.3. Climate dataset

Meteorological data on P, T, and SR at the monthly scales were collected at a spatial resolution of 0.25° × 0.25° from 01/2000 to 12/2015. The data collected from GLDAS-2.1 data sets of the National Aeronautics and Space Administration (NASA) (https://www.nasa.gov/) with the global spatial coverage (60S, 180 W, 90 N, 180E). Combining ground observation and satellite data products, GLDAS-2.1 generated optimal near real-time surface state variables by data assimilation, which had overcome the limitations of ground observation (Rodell et al., 2004). A large number of studies and evaluation results showed that GLDAS-2.1 data had high reliability (Kato et al., 2007; Li et al., 2018b; Piao et al., 2015). To ensure the computational accuracy, all meteorological data sets were sampled into a unified spatial resolution of 1 km (the same as the NPP data). The projection method adopted was Albers Conical Equal Area Projection (krasovsky-1940-albers).

3.4. Karst dataset

The karst boundary used in this study was the exposed karst area, not including covered and buried karst area. Carbonate rock outcrops (exposed karst area) of China were based on the v3.0 revision world map of carbonate rock outcrops obtained from Geography and Environmental Science, University of Auckland (http://www.sges.auckland.ac.nz/sges_research/karst.shtm). The region boundaries also came from this database. The area of carbonate rock-outcrops provided an upper limit on the area of exposed karst terrain (Li et al., 2018b). In order to make the karst boundary more accurate, the carbon rock outcrops data was integrated with the more detailed and complete exposed karst data of eight southern provinces (GZ, YN, CQ, HUN, HUB, GD, GX, and SC) provided by the Karst Scientific Data Center, Institute of Geochemistry, Chinese Academy of Sciences

(http://www.karstdata.com/). So, the karst area used in this study was approximately 1.88 million km^2, within which the area covered with vegetation was 1.51 million km^2.

4. Methods

4.1. Trend analysis

Linear tendency estimation was used to analyse the temporal dynamics of NPP and climatic factors, and statistical test of correlation coefficient was used to evaluate the significant change trend. With the time change, NPP and climatic factors tended to increase or decrease in the entire sequence, change in spatial distribution pattern and turn or mutate at a certain time. These variables could be considered as linear regression of time. The linear tendency value was estimated by using the least square method.

$$K = \frac{\sum_{j=1}^{n} M_j t_j - \frac{1}{n}\sum_{j=1}^{n} M_j \sum_{j=1}^{n} t_j}{\sum_{j=1}^{n} t_j^2 - \frac{1}{n}\left(\sum_{j=1}^{n} t_j\right)^2} \quad (1)$$

where K is the linear tendency value; n is the study period. j represents the year order; and M_j is the independent variable corresponding to year j. If the correlation coefficients of regression equation pass through the significant levels of confidence 0.05 and 0.01 ($p < 0.05$ and $p < 0.01$), then M_j decreases or increases to significant and extremely significant levels, respectively.

4.2. Partial derivatives for quantifying the impacts of climate and human-induced NPP variations

The target variables can been then partitioned into multiple components according to Eq. (2) on the support of Roderick et al. (2007), which has been widely applied into assessing the impacts of various interfering factor on hydrological and meteorological changes (You et al., 2013; Liu and Sun, 2016). Thus, the partial derivatives has been applied in an attempt to estimate the impacts of climate-driven factors to NPP variations:

$$\frac{dY}{dt} = \frac{\partial Y}{\partial X_a} \times \frac{dX_a}{dt} + \frac{\partial Y}{\partial X_b} \times \frac{dX_b}{dt} + \frac{\partial Y}{\partial X_c} \times \frac{dX_c}{dt} + \cdots + \frac{\partial Y}{\partial X_n} \times \frac{dX_n}{dt} = X_{a_{con}} + X_{b_{con}} + X_{c_{con}} + \cdots + X_{n_{con}} \quad (2)$$

where $\frac{dY}{dt}$ represents the linear trend of the Y variations, $X_{a_{con}}$, $X_{b_{con}}$, $X_{c_{con}}$, $X_{n_{con}}$, …, and $X_{n_{con}}$ represent the contributions of X_a, X_b, X_c, …, and X_n to Y variations, respectively. $\frac{\partial Y}{\partial X_a}$, $\frac{\partial Y}{\partial X_b}$, $\frac{\partial Y}{\partial X_c}$…, and $\frac{\partial Y}{\partial X_n}$ represents the partial derivatives of Y variations with various variables, respectively. From the definition of formula, the each partial derivatives equals the corresponding second-order partial correlation coefficient by eliminating the effect of the other two variables, respectively.

This study assumed that CC and HA were the main causes of vegetation NPP changes. The contributions of HA to vegetation NPP variations could be seen as the bias between the observed (K) and climatic estimated NPP (C_con) as follows,

$$K \approx C_{\_con} + H_{\_con} = T_{\_con} + P_{\_con} + SR_{\_con} + H_{\_con} = \frac{\partial NPP}{\partial T} \times \frac{dT}{dt} + \frac{\partial NPP}{\partial P} \times \frac{dP}{dt} + \frac{\partial NPP}{\partial SR} \times \frac{dSR}{dt} + H_{con} \quad (3)$$

where K is the change trend of NPP resulted from the interaction of CC and HA, which is obtained from Eq. (1); *C_con* is the contribution of CC, representing the sum of T_con, P_con, and SR_con; *H_con* is the contribution of HA, which equals the residual between K and C_{con}. T_con, P_con, and SR_con is the contribution of T, P, and SR to NPP variations, respectively. Here, T, P and SR were considered as the main climatic factors. Given that all types of factors have a linear influence on the change in NPP, the second-order partial correlation coefficient between one factor and NPP could be obtained by eliminating the other two factors separately. The second-order partial correlation coefficients were calculated as follows (Xu et al., 2010):

$$R_{xy,z\lambda} = \frac{R_{xy,z} - R_{x\lambda,z} \times R_{y\lambda,z}}{\sqrt{(1 - R^2_{x\lambda,z}) \times (1 - R^2_{y\lambda,z})}} \quad (4)$$

where $R_{xy,z\lambda}$ represents the second-order partial correlation coefficient between x and y by eliminating the impact of factors z and λ; $R_{x\lambda,z}$ and $R_{y\lambda,z}$ have similar definitions to $R_{xy,z}$ as above. Judging the significance of the relevance of two variables by t-test. If p is less than 0.05, it will pass the 95% confidence significance test, otherwise, it will not be significant.

4.3. Eight scenarios for assessing the contribution proportions of climate and human-induced NPP variations

By consider in the complexity of each driving mechanism, eight scenarios supported by previous studies (Li et al., 2016; Xu et al., 2010; Yan et al., 2019; S. Zhou et al., 2017; W. Zhou et al., 2017; Zhou et al., 2015) were set up in Table 1 on the basis of K, C_con, and H_con to estimate the contributions that CC and HA contribute to NPP increasing and decreasing against the background of ambitious afforestation in karst areas of China. Here, it was defined as “climate-controlled NPP increasing or decreasing” in the case of the contribution proportion of CC to NPP increasing or decreasing exceeded that of HA. Otherwise, it was defined as “human-controlled NPP increasing or decreasing”.

Note: Scenario 1 or 5: NPP increasing or decreasing resulted from the disturbance of CC and HA; Scenario 2 or 6: Climate-controlled NPP increasing or decreasing; Scenario 3 or 7: Human-controlled NPP increasing or decreasing; Scenario 4 or 8: Two scenarios that can not happen for NPP increasing or decreasing.

4.4. Calculation of net NPP increasing areas

To further clarify the net contributions caused by CC and HA to regional NPP variations, the proportions of net NPP increasing areas

Table 1
Eight scenarios for quantitatively assessing the contribution proportions of climate-and human-controlled NPP increasing or decreasing.

	K	Scenario	C_con	H_con	Contribution of CC (%)	Contribution of HA (%)
NPP increasing	K > 0	Scenario 1	> 0	> 0	$\frac{\lvert C\_con\rvert}{\lvert C\_con\rvert + \lvert H\_con\rvert} \times 100$	$\frac{\lvert H\_con\rvert}{\lvert C\_con\rvert + \lvert H\_con\rvert} \times 100$
		Scenario 2	> 0	< 0	100	0
		Scenario 3	< 0	> 0	0	100
		Scenario 4	< 0	< 0	Impossible	Impossible
NPP decreasing	K < 0	Scenario 5	< 0	< 0	$\frac{\lvert C\_con\rvert}{\lvert C\_con\rvert + \lvert H\_con\rvert} \times 100$	$\frac{\lvert H\_con\rvert}{\lvert C\_con\rvert + \lvert H\_con\rvert} \times 100$
		Scenario 6	< 0	> 0	100	0
		Scenario 7	> 0	< 0	0	100
		Scenario 8	> 0	> 0	Impossible	Impossible

(NNIA) that CC and HA contributed to NPP variations and the total NNIA of both were calculated as follows:

$$S_{NNIA} = S_{CC_{NNIA}} + S_{HA_{NNIA}} \quad (5)$$

$$S_{CC_{NNIA}} = S_{CC_{Increasing}} - S_{CC_{Decreasing}} \quad (6)$$

$$S_{HA_{NNIA}} = S_{HA_{Increasing}} - S_{HA_{Decreasing}} \quad (7)$$

where S_{NNIA} is the total net NPP increasing areas that CC and HA contributed to NPP variations; $S_{CC_{NNIA}}$ is the net NPP increasing areas that CC contributed to NPP variations; $S_{HA_{NNIA}}$ is the net NPP increasing areas that CC contributed to NPP variations; $S_{CC_{Increasing}}$ is the areas that CC contributed to NPP increasing; $S_{CC_{Decreasing}}$ is the areas that CC contributed to NPP decreasing; $S_{HA_{Increasing}}$ is the area that HA contributed to NPP increasing; $S_{HA_{Decreasing}}$ is the area that HA contributed to NPP decreasing.

5. Results

5.1. Spatial distribution in NDVI and NPP

The average NDVI value in the vegetation-covered karst (VCK) areas was 0.52 (Fig. S1) and the average NPP value in this areas was 411.94 g C m^{-2} yr^{-1} during 2000–2015 (Fig. S2). Overall, the average NDVI and NPP values showed the prominently decreased trend from south to north and east to west. The average NDVI value was higher than 0.6 in most karst areas in southern and northern China, but lower than 0.4 in karst areas of the Qinghai-Tibet Plateau. The areas with high NPP values were mainly distributed in eight southern provinces (on regional average was 676.31 g C m^{-2} yr^{-1} over SC, CQ, GZ, YN, GD, GX, HN, and HUB). Notably, the largest NPP value was located in HAN (998.46 g C m^{-2} yr^{-1}) despite very small karst area distributed in this province (Fig. S2). By contrary, the lowest average NPP value was identified in TB (54.07 g C m^{-2} yr^{-1}) with large karst areas. Viewed from karst zones, the areas with low NPP values were primarily distributed in karst areas of northern China (270 g C m^{-2} yr^{-1}) and the Qinghai-Tibet Plateau (108 g C m^{-2} yr^{-1}). Obviously, the average NPP value was relatively higher (653.38 g C m^{-2} yr^{-1}) in southern karst area, which was 2.5 times than that in northern karst area, 6 times than that in karst areas of the Qinghai-Tibet plateau and 1.6 times than that of the entire VCK area. Thus, the spatial distribution of average NPP was very similar to that of average NDVI in karst areas of southern China and the Qinghai-Tibet Plateau.

5.2. Temporal-spatial changes in NDVI and NPP

The NDVI over the entire VCK area exhibited an unremarkable increasing trend at a rate of 0.004 yr^{-1} ($p > 0.05$) during 2000–2015 (Fig. 2a). In the entire VCK area, the area of NDVI significantly increased was 1.35 million km^2, accounting for 88.93% of VCK area (59.76% for significant increase and 29.17% for insignificant increase), while the area of NDVI decreased was only 0.17 million km^2, accounting for 11.07% of VCK area (9.88% for insignificant decrease and 1.19% for significant decrease) (Fig. 2b). This indicated that the vegetation in most karst areas exhibited a significant greening trend (mainly distributed in southern and northern karst areas), but only in northwestern TB, the vegetation showed a yellowing trend. For three divided karst zones, the highest NDVI increasing rate was obtained in southern karst area (0.0054 yr^{-1}, $p > 0.05$), followed by northern karst area (0.0053 yr^{-1}, $p > 0.05$), and the lowest was observed in karst area of the Qinghai-Tibet Plateau (0.002 yr^{-1}, $p > 0.05$). In space, the fastest growing area of NDVI was observed at the junction of YN-GZ-SC and SX. However, the areas with the most evident NDVI decline were observed in karst areas of northwestern TB. Furthermore, the increasing trends in NDVI were observed in all karst provinces (Table S1), whereas the significant increasing trends of NDVI were observed in BJ, SX, JL, HLJ, and SAX.

The average NPP over the entire VCK area exhibited an unremarkable increasing trend at a rate of 0.92 g C m^{-2} yr^{-1} ($p > 0.05$) during 2000–2015 (Table S1). For three divided karst zones, the highest NPP increasing rate was obtained in northern karst area (2.56 g C m^{-2} yr^{-1}, $p > 0.05$), followed by the karst area of the Qinghai-Tibet Plateau (1.17 g C m^{-2} yr^{-1}, $p < 0.01$), and the lowest was observed in southern karst area (0.34 g C m^{-2} yr^{-1}, $p > 0.05$). The karst area of Qinghai-Tibet Plateau and northern China contributed 81.98% and 83.55% of their areas for NPP increasing respectively, and these regions contributed 66.31% of NPP growth area in the entire VCK area. Although NPP overall increased in different karst zones and VCK area, the variation trend of it presented distinct spatial difference. Not only did NPP decrease in one third of the VCK area (33.69%), but also in approximately half (47.58%) of the southern karst areas (Fig. 2c). Moreover, 17.02% for the VCK area exhibited the prominently decreasing trend ($p < 0.05$), and 48.28% of which was contributed by the southern karst areas (Fig. 2d). In space, the fastest growing area of NPP was located at the junction of YN-GZ-SC and YN-SC-TB. However, the areas with the most evident NPP decline were located in karst areas of eastern GZ and northern GX. Furthermore, the increasing trend in NPP were observed in most provinces of northern China (Table S1), whereas the insignificant decreasing trends of NPP were observed in FJ, HUN, GD, GX, and GZ. Specially, the largest areas with NPP decreasing was obvious observed in GZ, followed by GX, TB and HUN.

5.3. Evolution relationship between NDVI and NPP

The evolution trends of NDVI were not consistent with that of NPP in some areas from the above analysis. Although there were similar change trends with an area of 0.98 million km^2 (64.46%) for NDVI and NPP, it was found that NPP showed a downward trend in the areas where NDVI increased with an area of 0.44 million km^2 (29.07%), and there were even some regions with the area of 9.78 km^2 in which NDVI decreased while NPP increased, which were primarily concentrated in karst areas of GZ, GX, GD and HUN. In addition, 16 evolution types coupled with the change trends of NDVI and NPP had been identified in Fig. 3, within which three obvious coupled types accounted for a large proportion (66.26%), respectively. The coupled type of NDVI significantly increased with NPP insignificantly increased showed the largest area of 0.45 million km^2, accounting for 29.54% of VCK area, followed by the coupled type of NDVI significantly increased with NPP insignificantly decreased, and the coupled type of NDVI increased insignificantly with NPP increased insignificantly, accounting for 19.31% (0.29 million km^2) and 17.41% (0.26 million km^2) of VCK area, respectively. Other coupled types had relatively small distribution areas (the total area was only 0.51 million km^2). These results indicated that vegetation turning green in some karst areas did not mean the increasing in vegetation productivity.

5.4. Contributions of CC and HA to vegetation NPP variations

The contributions of T, P, and SR to NPP variations showed a significant spatial differences in the VCK area (Fig. S3). Overall, SR obtained the largest negative contribution in the entire VCK area (-0.91 g C m^{-2} yr^{-1}) during 2000 to 2015, whereas P obtained a positive contribution (0.25 g C m^{-2} yr^{-1}), and T made the smallest positive contribution (0.04 g C m^{-2} yr^{-1}) (Table 2). Moreover, the contributions of three climatic factors to NPP variations also showed different distributions in three divided karst regions. SR obtained the largest negative contribution in karst areas of southern China, but showed a higher positive contribution in the Qinghai-Tibetan plateau and northern China. P only made a higher negative contribution in karst areas of the Qinghai-Tibetan plateau. Notablely, T demonstrated a

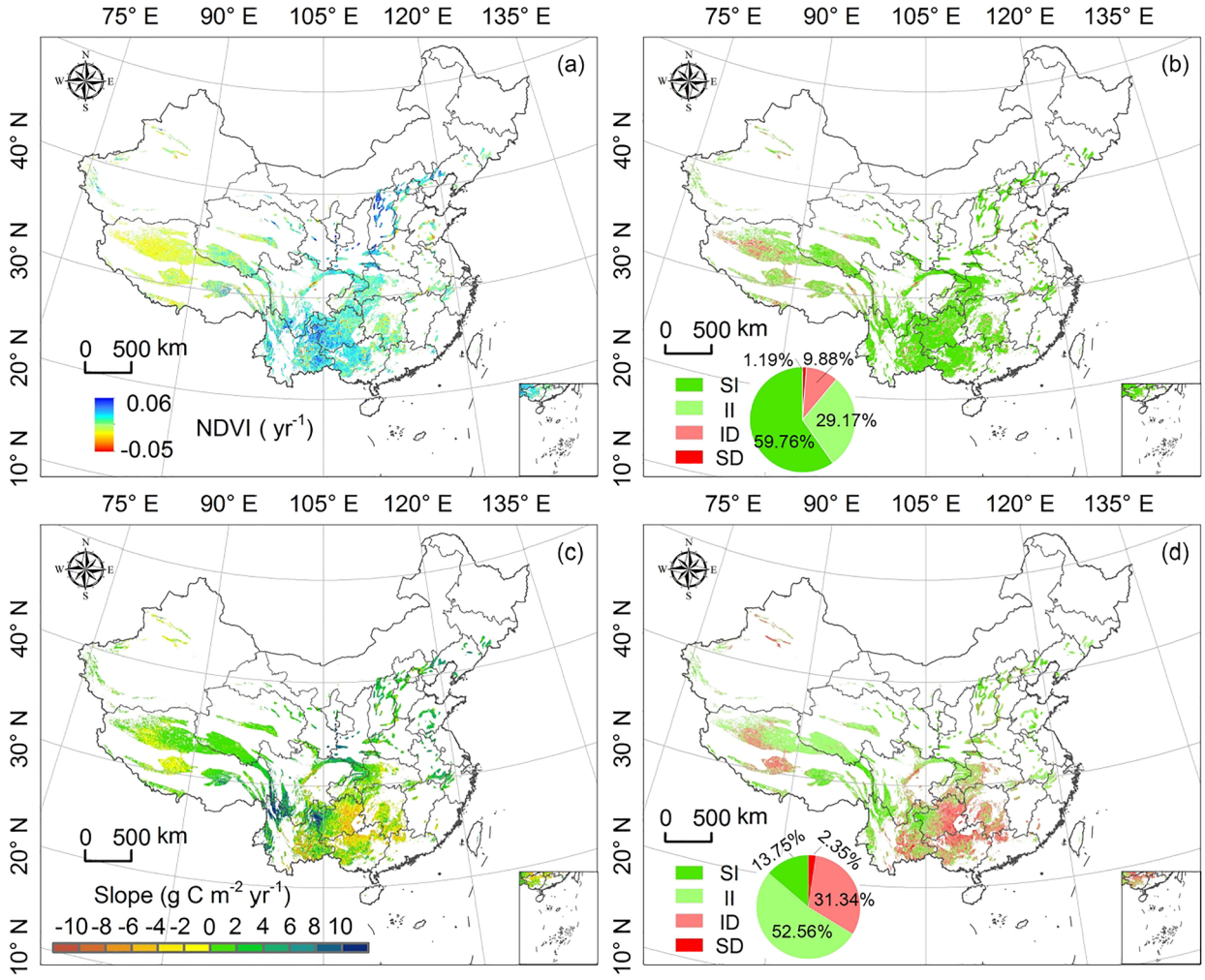

Fig. 2. Variation trend and significant levels for NDVI (a, b) and NPP (c, d) in karst areas based on spatial pixel during 2000 to 2015. The SI, II, ID, and SD in (b, d) represents the change degree of significant increase, insignificant increase, insignificant decrease, and significant decrease in (a, c) respectively.

small positive contribution in the Qinghai-Tibetan plateau and northern China and a small negative contribution in most southern karst areas.

To determine the main climatic factors that controlled NPP variations in karst areas, the climatic factor with the largest absolute contribution on the pixel was selected as the main influence factor for NPP variations. As shown in Fig. S3d, the areas dominated by T_con, P_con, and SR_con account for 0.16% (2494.29 km^2), 26.64% (0.403 million km^2), and 73.20% (1.11 million km^2) of the total VCK area, respectively. The areas dominated by SR and P accounted for 99.84% of the total VCK area, thereby indicating that they were the two main factors that affected the annual NPP variation in karst areas. P was critical to NPP increasing in karst areas of northern China and the junction of YN, GZ, and SC. The increased SR accelerated the NPP accumulation in karst areas of the Qinghai-Tibet Plateau and northern China, but the decreased SR led to the sharp decrease in NPP in eastern GZ, HUN, CQ, YN, and northern GX.

Furthermore, the contributions caused by CC and HA to NPP changes were obtained based on Eq. (3) (Fig. 4). We obtained a surprise discovery that the regions with the greater negative contribution of CC to NPP changes were also the regions with the greater positive contribution of HA, such as GZ, GX, CQ and HUN, which indicated that the government was trying to offset the negative effects of CC on vegetation productivity restoration through ecological projects over the years. Although HA contributed positively to NPP increasing, CC showed greater negative impact on it, which resulted in the positive impact of HA in most karst areas in southern China was greatly weakened by the negative impact of CC. For the VCK areas, the areas where NPP changes controlled by CC and HA were 0.87 (60% for NPP increasing and 40% for NPP decreasing) and 0.64 million km^2 (75% for NPP increasing and 25% for decreasing), which accounted for 57.62% and 42.39% of the total VCK areas, respectively. It was showed that CC (-0.61 g C m^{-2} yr^{-1}) caused a negative contribution to NPP variations in VCK areas (Table 2), whereas HA (1.53 g C m^{-2} yr^{-1}) obtained the largest positive contribution. For the three divided karst zones, HA (2.85 g C m^{-2} yr^{-1}) caused a larger positive contribution, whereas CC (-2.51 g C m^{-2} yr^{-1}) caused a negative contribution in southern karst zones. Obviously, CC demonstrated a larger positive contribution (0.77 g C m^{-2} yr^{-1}) than that of HA (0.40 g C m^{-2} yr^{-1}) in karst zones of the Qinghai-Tibetan Plateau. Specially, a positive contribution made by CC (3.27 g C m^{-2} yr^{-1}) and a negative contribution made by HA (-0.71 g C m^{-2} yr^{-1}) to NPP variations were identified in northern karst area, respectively, which were contrary to that in southern karst area. For provinces, CC obtained more positive contributions in most northern provinces and the Qinghai-Tibetan plateau, whereas HA demonstrated more positive contributions in most southern provinces.

5.5. Contribution proportions of CC and HA contribute to NPP increasing and decreasing

To further accurately identify the dominant areas of each influencing factor, the contribution proportions of CC and HA for NPP increasing and decreasing were calculated according to the eight different

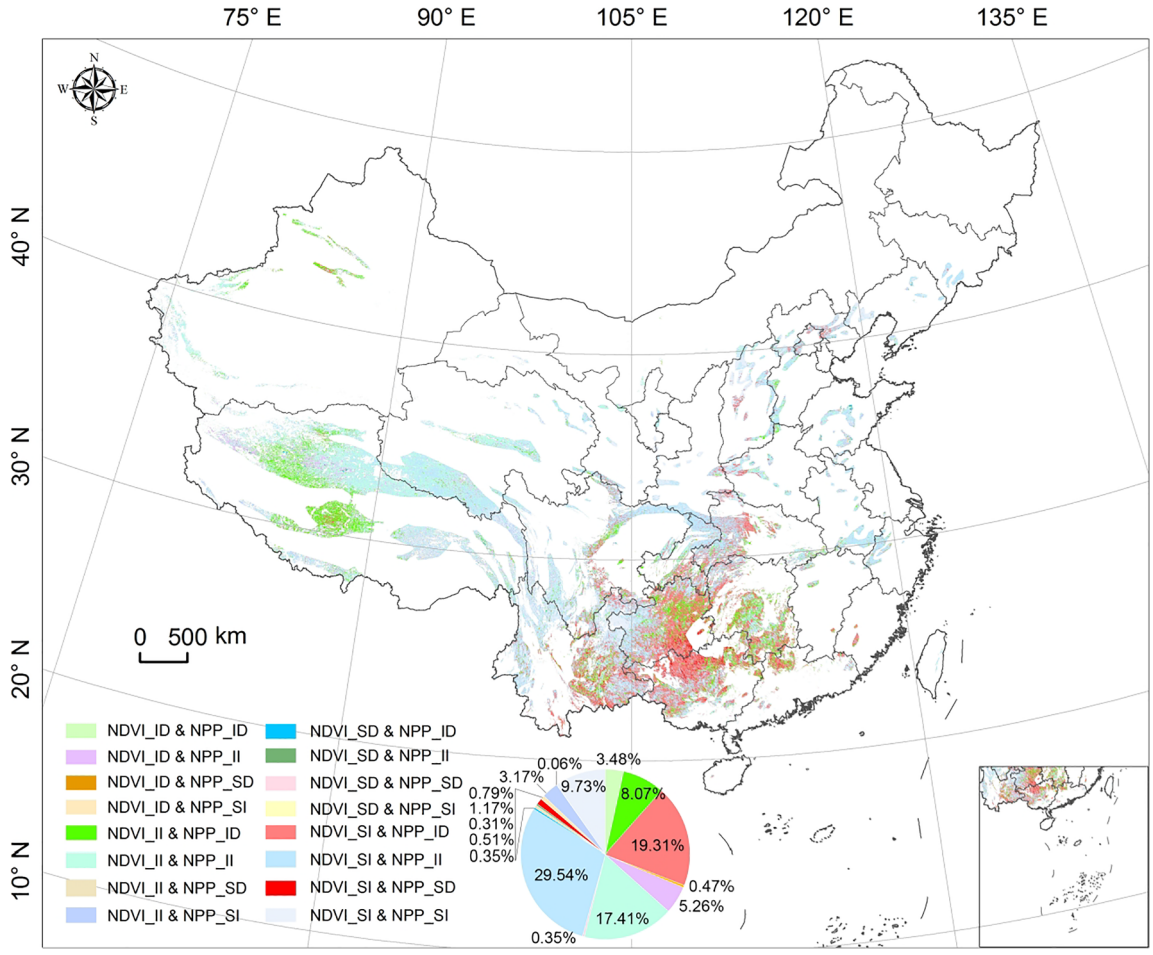

Fig. 3. NPP change trends combined different NDVI change characteristics in karst areas of China. The SI, II, ID, and SD represent the variety characteristics in significant increase, insignificant increase, insignificant decrease, and significant decrease, respectively.

designed scenarios in Table 1. As shown in Fig. 5. The contribution proportions of dominant factors for NPP increasing and decreasing exhibited significant spatial differences. For entire VCK areas, the percentages of climate- and human-controlled accounted for 51.94% and 48.06% for NPP increasing (Fig. 5a, b), whereas 68.43% and 31.57% for NPP decreasing (Fig. 5c, d), respectively. Thus, CC and HA showed the more similar contribution proportion for NPP increasing, but with great difference for NPP decreasing. In southern karst areas, CC dominated the NPP decreasing (70.72%) mainly located in eastern GZ, northern GX, southern HUN, and the border area along GZ, CQ, and HUN (Fig. 5e, f). HA dominated the NPP increasing (59.07%) in southern karst areas, mainly located in YN, the border area between GZ and SC, central GX, central and southern HUN, and the border area along YN, GZ, and GX. By contrast, in northern karst area, CC was the

Table 2
Regional average contribution values caused by CC and HA to NPP variations in different provinces and karst zones (g C m^{-2} yr^{-1}).

Region	T	P	SR	CC	HA	Region	T	P	SR	CC	HA
Karst	0.04	0.25	−0.91	−0.61	1.53	HN	0.01	−0.62	5.16	4.55	−2.87
Southern China	0.01	0.42	−2.95	−2.51	2.85	HUB	0.01	−1.79	0.11	−1.68	2.31
Qinghai-Tibetan Plateau	0.10	−0.31	0.98	0.77	0.40	HUN	0.02	−0.09	−7.97	−8.04	6.92
Northern China	0.02	1.12	2.13	3.27	−0.71	GD	0.00	0.09	2.26	2.34	−4.13
BJ	0.01	2.15	0.22	2.38	−1.10	GX	0.00	−0.75	−4.38	−5.13	3.61
TJ	0.04	3.44	1.60	5.08	−1.99	HAN	0.00	−6.11	0.86	−5.26	5.48
HB	0.02	2.00	0.83	2.85	−0.67	CQ	0.02	0.62	−4.52	−3.89	5.08
SX	0.03	2.11	1.10	3.24	−0.33	SC	0.04	0.81	−0.40	0.45	2.09
IM	0.04	2.22	0.54	2.81	−0.60	GZ	0.01	0.16	−6.94	−6.77	5.97
LL	0.04	1.96	2.15	4.15	0.87	YN	0.01	1.39	0.42	1.82	0.52
JL	0.01	1.20	−1.26	−0.05	3.87	TB	0.10	−0.81	1.51	0.80	−0.14
HLJ	0.00	−0.09	9.24	9.15	−5.39	SAX	0.01	0.62	4.50	5.13	−0.58
JS	0.01	1.02	5.48	6.50	−2.54	GS	0.04	0.64	0.53	1.22	1.49
ZJ	−0.01	11.61	0.66	12.27	−9.45	QH	0.11	0.20	−0.58	−0.27	0.96
AH	0.00	5.00	3.16	8.16	−4.32	NX	0.04	1.76	5.70	7.49	−2.07
FJ	0.00	−1.99	−0.25	−2.25	−0.20	XJ	0.02	0.39	1.00	1.41	−1.11
JX	0.01	3.98	−0.07	3.91	−3.58	TW	0.00	−1.06	7.27	6.20	0.34
SD	0.02	−0.20	6.14	5.95	−2.42	–	–	–	–	–	–

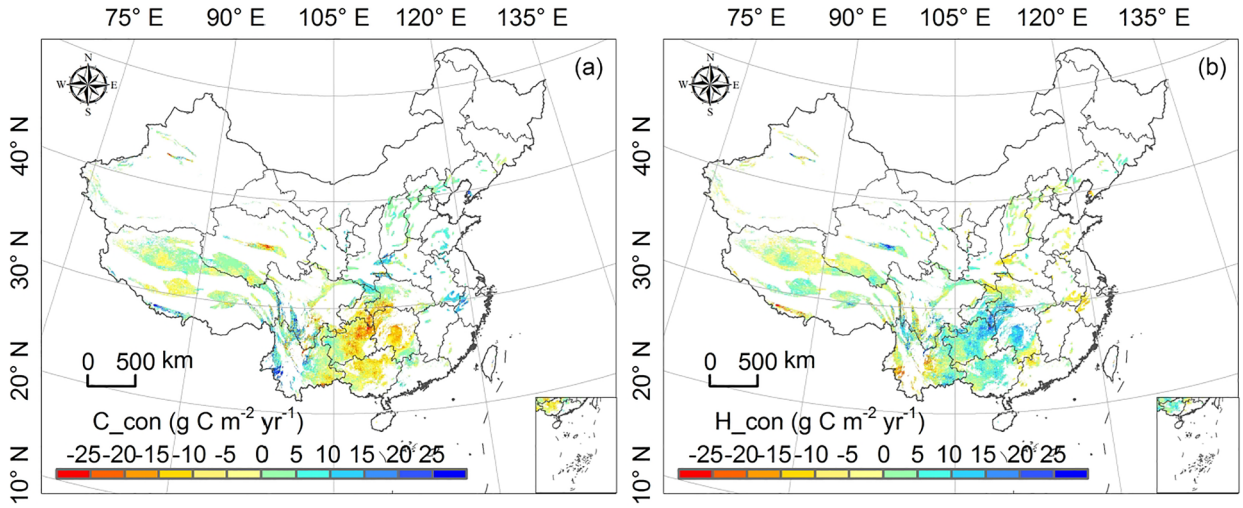

Fig. 4. The contributions caused by CC (C_con) (a) and HA (H_con) (b) to NPP variations in space.

main cause of NPP increasing (71.98%), whereas HA dominated the NPP decreasing (57.19%). Unexpectedly, CC was the main controlling factor for NPP increasing (52.84%) and decreasing (67%) in karst areas of the Qinghai-Tibetan plateau.

For provinces, CC dominated NPP increasing in northern provinces (Fig. 6a). However, the increasing of NPP in southern provinces was mainly attributed to HA (mainly ecological afforestation projects) while the negative effects of CC had led to a large area of NPP decline in this region (Fig. 6b). NPP decline in northern provinces was mainly caused by HA. Thus, a large number of ecological projects had promoted the growth of NPP in southern provinces where karst was concentrated, but the negative effect of CC had also led to a large reduction of NPP in this region.

5.6. The net change areas in NPP

As shown in Fig. 6c, the total NNIA of CC and HA was 0.49 million km^2, which accounted for 32.62% of the VCK area. The proportion of NNIA dominated by HA accounted for 65.09% of the total NNIA in the VCK area, whereas that dominated by CC was only 34.91%. The proportions of NNIA dominated by CC (52.84%) and HA (47.16%) were higher in karst areas of the Qinghai-Tibet Plateau. 58.29% of NNIA was dominated by HA and −41.71% of it was dominated by CC in southern karst area, whereas 20.86% and 79.14% of NNIA were dominated by HA and CC in northern karst area, respectively. Hence, HA dominated NNIA in southern karst areas while CC controlled NNIA in northern karst areas. Among the provinces, CC dominated a relatively higher proportion of NNIA in most northern provinces, while it dominated lower proportion of NNIA in southern provinces. By contrary, the proportion of NNIA controlled by HA was relatively higher in CQ (95.40%), SC (64.74%), HUB (65.87%), HAN (56.91%) and YN (54.16%), but relatively lower in GZ (33.31%), GX (24.02%), mainly due to the negative effects of CC.

For the total NNIA, the largest proportion of NNIA at 68.05% was contributed by karst area of the Qinghai-Tibet Plateau with lower NPP, whereas the lowest proportion of NNIA at 7.96% was observed in southern karst area with higher NPP. Among the provinces, the lowest NNIA of −0.07 million km^2 was identified in GZ and GX. Surprisingly, the largest proportion of NNIA was observed in TB (34.02%) and QH (22.82%). It could been seen that the positive contribution of HA to NPP changes was largely offset by the negative effect of CC in karst area of southern China.

6. Discussion

6.1. Comparison of quantitative evaluation methods on vegetation productivity

Quantifying the impacts that CC and HA contributed to NPP variations had traditionally been a challenge due to the complexity and uncertainty of driving mechanisms. In the past, many mathematical statistical method, such as linear regression, Lindeman-Merenda-Gold method, variance decomposition, principal component analysis, residual trend, and multivariable analysis, were commonly used methods to evaluate the relative contributions of driving factors (Gollnow and Lakes, 2014; Herrmann et al., 2005; Jiang et al., 2017; Ma et al., 2007; Millington et al., 2007; Schweizer and Matlack, 2014; Ye et al., 2019; S. Zhou et al., 2017; W. Zhou et al., 2017). However, these statistical techniques were often criticized for failing to accurately identify the effect of HA. Recently, some researches were conducted to separate vegetation carbon increment caused by human activity from multiple influencing factors by comparing the actual climate-driven aboveground biomass change without anthropogenic influence via the LPJ-GUESS ecosystem model (Smith et al., 2014) and Miami models (Adams et al., 2004; Krausmann et al., 2009; S. Zhou et al., 2017; W. Zhou et al., 2017; Zhou et al., 2015), which defined the potential NPP (or biomass) on the basis of potential vegetation by fixing a climate condition or setting up a variety of climate scenarios. Nevertheless, there was high uncertainty in the simulation results.

This study aimed to separate effectively and assess quantitatively the impact of CC and HA on the vegetation productivity evolution. We attempted to select NPP as an indicator to represent vegetation productivity on the support of studies of Roderick et al. (2007) and Xu et al. (2010) and selected T, P, and SR as the evaluation indicators of main climatic factors. Then, the contributions caused by CC and HA to vegetation productivity were quantitatively evaluated by using the partial derivatives. Lastly, the contribution proportions of CC and HA to NPP increasing and decreasing were also evaluated by setting up eight different scenarios with consideration for the complexity of driving mechanisms.

Moreover, CO_2 fertilisation, which seemed to remarkably affect on the plant growth (Braswell, 1997; Mu et al., 2008; Myneni et al., 1997; Zhu et al., 2016), was included in HA in this study. Although previous researches found that the CO_2 fertilisation showed a significant effect on vegetation growth in hot and arid environments where plant growth was limited by water (Chen et al., 2019a; Donohue et al., 2013;

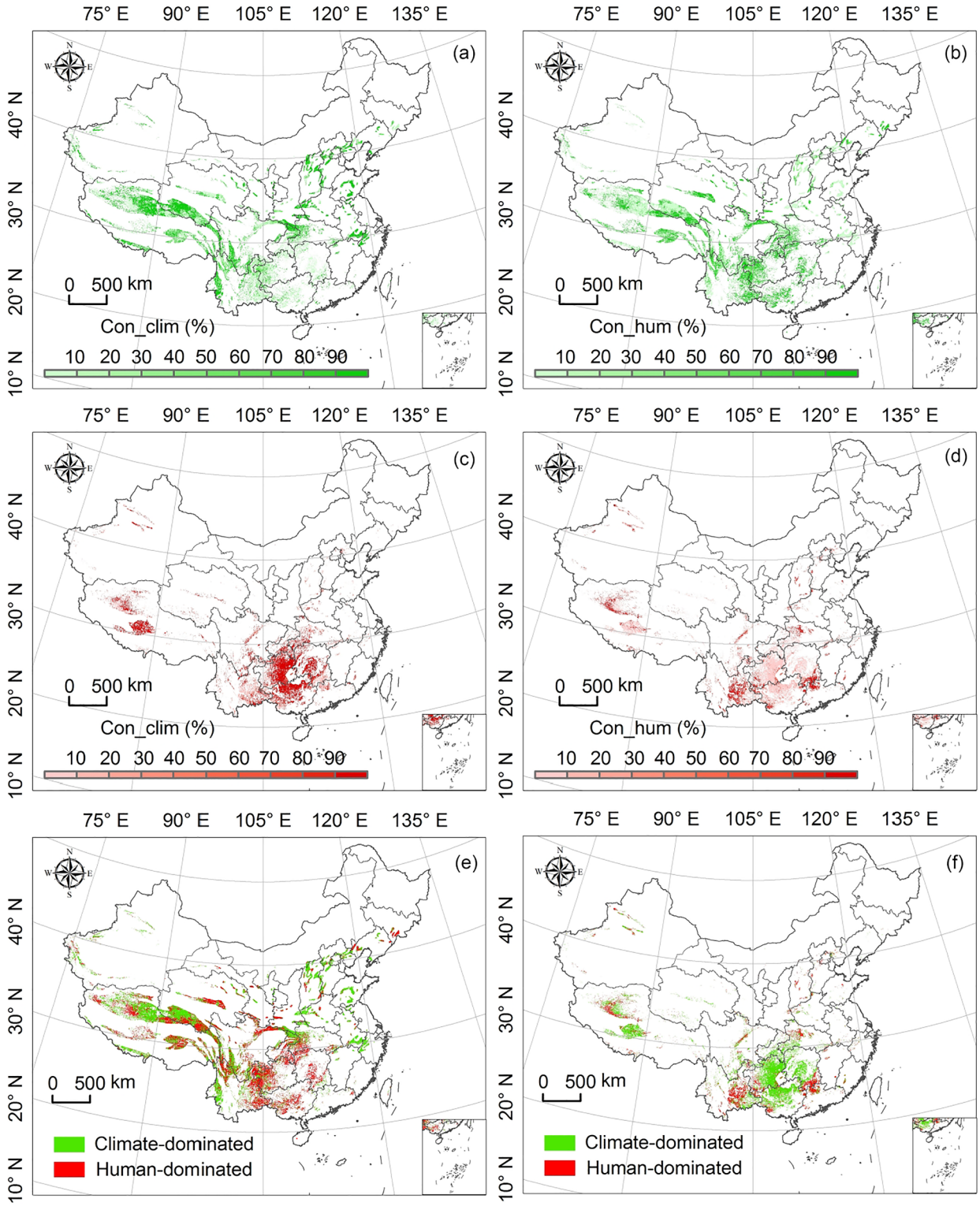

Fig. 5. The impact of CC and HA on NPP changes. The contribution proportions that CC (Con_clim) (a) and HA (Con_hum) (b) contributed to NPP increasing; The contribution proportions that CC (Con_clim) (c) and HA (Con_hum) (d) contributed to NPP decreasing; Spatial distributions of the climate- and human-dominated NPP increase areas (e) and decrease areas (f).

Mcmurtrie et al., 2008), such effects had the weakest impact on vegetation in the arid environments of northwest China (Mu et al.,2008), even in all China (Xiao et al., 2015; Piao et al., 2018). Moreover, it was said that CO_2 fertilisation effects explained most of the greening trends in the tropics, whereas it was not CO_2 fertilisation, but CC resulted in greening in the regions of high latitudes and the Qinghai-Tibet Plateau (Zhu et al., 2016). Meanwhile, recent researches suggested land use change dominated by HA (afforestation projects) contributed most to the regional greening, which was clearly observed in southwestern China (Piao et al., 2015; Zhu et al., 2016). Overall, it could be seen that HA was the key role in the residual factors.

The advantage of this method was that the uncertainty of simulated

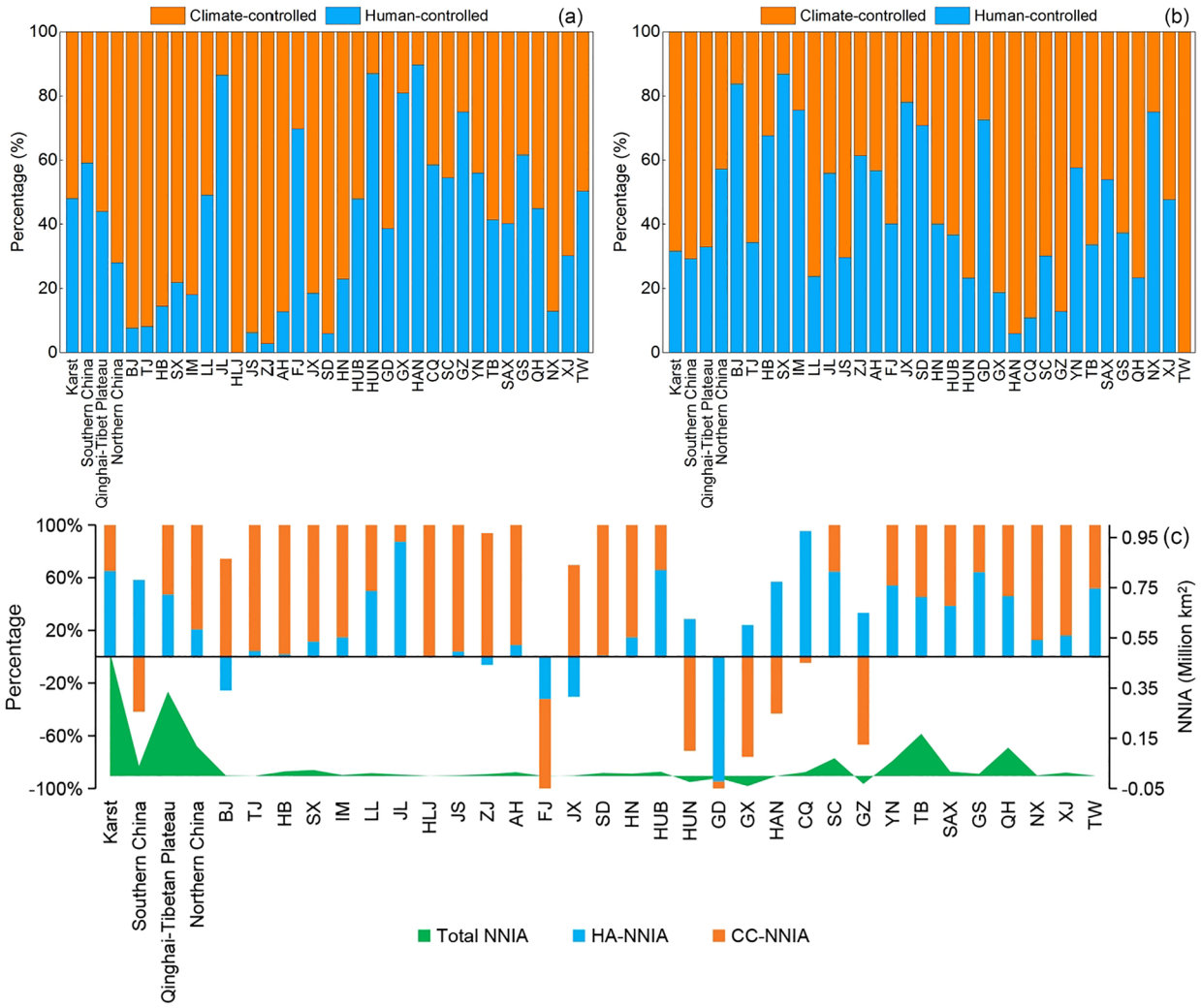

Fig. 6. Statistical results of contribution proportions and NNIA controlled by CC and HA to NPP changes in different provinces and karst zones. (a) The contribution proportions of climate- and human-controlled NPP increasing; (b) The contribution proportions of climate- and human-controlled NPP decreasing; (c) The percentages of climate- and human-controlled NNIA and the total NNIA.

potential NPP by using Miami model used in previous studies could be effectively avoided. Moreover, the impact of any actuation factor associated with CC and HA capable of being effectively decomposed and accurately calculated regardless of how complex the relationship among the factors was, even if their expression was unknown. Therefore, this method was capable of quantitatively analyzing the evolution process of vegetation productivity and its driving factors in karst areas, and could be widely used in the researches on eco-hydrological process.

6.2. Comparisons of the results with that in previous studies

We compared our results with previous researches (the study area included karst area and non-karst area) from different regions and found some differences.

For the grassland NPP changes in China, the contributions of CC and HA to NPP decrease were almost equilibrium (47.9% vs 46.4%). But for the NPP increase, HA was the dominant driving factors (78.1% for HA and 21.9% for CC) (S. Zhou et al., 2017; W. Zhou et al., 2017). In our study, CC and HA showed the more similar contribution proportion for NPP increase (51.94% vs 48.06%) for the entire VCK (vegetation-covered karst area) areas, but with great difference for NPP decrease (68.43% vs 31.57%). The two studies were relatively consistent in the recognition of contributions of CC and HA to NPP changes.

For the grassland NPP changes in northern China, the role of HA in both NPP increase (55.79%) and decreasing (74.83%) was the main control factor (Yan et al., 2019). This result that HA was the main control factor for NPP changes was consistent with the result of Zhou et al. (2015), who concluded that 69% of NPP decrease was caused by HA compared with 15.2% induced by CC, and 23.9% of NPP increase was caused by CC, whereas 54% resulted from HA in the northwest China. But, this view was different from our result that CC was the main cause of NPP increase (71.98%), whereas HA dominated the NPP decreasing (57.19%) in northern karst area.

For the grassland NPP changes in the Qinghai-Tibet Plateau, 56.7% of the NPP reduced areas was influenced by CC, and 19.9% was affected by HA. But HA was the dominant driving factors for NPP increasing (Wang et al., 2016). However, in our study, CC was the main controlling factor for NPP increasing (52.84%) and decreasing (67%) in karst areas of the Qinghai-Tibetan plateau. For the southern karst areas, this study suggested that CC dominated the NPP decreasing (70.72%) and HA dominated the NPP increasing (59.07%) in southern karst areas. This view was consistent with the latest study that had found a large increase in carbon sequestration of which about half was caused by newly planted and managed forests (Tong et al., 2020).

For provinces, most studies suggested that the relative roles of two factors possessed great spatial heterogeneity in all provinces (Forkel et al., 2014; Huang et al., 2018; X. Liu et al., 2019; Y. Liu et al., 2019;

Piao et al., 2015; Wang et al., 2016; Zeng et al., 2018). In one province, the difference of contribution of CC between in karst and non-karst areas was mainly caused by the spatial heterogeneity of climate factors such as precipitation, radiation, and temperature, etc. The difference of contribution of CC between regions was related to the change characteristics of climate factors. But, the difference of HA might be larger, which was mainly because the ecological projects were mainly implemented in the karst area (Tong et al., 2018; Delang and Yuan, 2015), while the intensity of implementation in the non karst area was relatively small. So the contribution of HA in karst area was higher than that in non-karst area. In our study, It also found that there were some differences of contribution values caused by CC and HA for the same province. As shown in Fig. 4 and Fig. 5, it was obvious that there were some differences of main control factors for NPP changes in karst areas of each province. CC dominated NPP increasing while HA dominated NPP decreasing in northern karst provinces. However, the increasing of NPP in southern karst provinces was mainly attributed to HA (mainly ecological afforestation projects) and the negative effects of CC had led to a large area of NPP decline in the region.

6.3. Effect of CC on vegetation productivity

In recent decades, lots of trees were planted by several large-scale afforestation projects in southern karst areas (Brandt et al., 2018b; Chen et al., 2019a). Biomass accumulated rapidly due to vegetation growth (Tong et al., 2018). However, we found that NPP decrease was most evident in southern karst areas, especially in GZ, GX, and HUN, which was the largest areas of net NPP reduction despite abundant hydrothermal conditions. This result supported the previous conclusion that NPP showed a slow downward trend in northeastern Guilin and Liuzhou of GX (Li et al., 2018), and even the downward trend was less than -0.05 g C m^{-2} yr^{-1} in certain areas (Li et al., 2014).

Previous researches had found that the interactions of T, water and light showed different effects on plant growth in different regions (Nemani et al., 2003). Lower P was the main constrain factor for vegetation productivity increasing in northern China (Yan et al., 2019). In forests, plant growth was often delayed by insufficient light. The lack of light became a major limiting factor for plant growth (Zhu et al., 2007), especially when the cloud cover was considerable and the duration was long (i.e., GZ, GX, CQ, and HUN, etc). In our study, we got a consistent finding that SR obtained a larger contribution value to NPP variations than T or P in most karst areas (73.20%), especially in southern karst area (Table S1d). Among all provinces, P contributed to the largest positive contribution to NPP variations in most provinces (i.e., SX, HB, AH, ZJ) where the increasing P reduced the restriction of water on vegetation growth and significantly promoted photosynthesis efficiency.

Although climatic stress was loosening in global (Nemani et al., 2003), the NPP growth in southern karst region was continuously hindered by the severe negative effects of SR. CC dominated the NPP decreasing in karst areas of southern China (i.e., eastern GZ, northern GX, and southern HUN) (Fig. 5c), owing mainly to increased cloud cover caused by increased P that resulted in the rapid reduction in SR (Nemani et al., 2003; Gonsamo et al., 2016). In that case, vegetation growth was constrained by a short-growing season length under these circumstances. This result confirmed the findings of Zhu et al. (2007), who assumed that NPP increasing in most areas of east and south China (29% of China's total land area) was mainly limited by light stress and also indicated that the higher NPP value raised the higher requirements of water and heat allocation conditions. Therefore, despite P increased in southern karst region, the lack of sunlight gave lower energy and subsequently caused an imbalance of water and heat conditions, which remarkably inhibited the time and efficiency of photosynthesis of vegetation and hindered carbon sequestration. However, although P showed a decreasing trend in karst region of YN (Fig. 7a), CC played a strong role in NPP recovery due to obvious higher SR than that in other areas in southern China (Fig. 7e, f). This finding was contrary to the case in the Amazon rainforest where 42% of NPP increasing benefit from increased SR caused by reduced cloud amount (Nemani et al., 2003). The negative contribution of CC to NPP variations in southern karst region was basically consistent with that of Tong et al. (2018), who found that the above-ground biomass and leaf area index simulated from the ecosystem model LPJ-GUESS without human disturbance (2000–2015) were declining due to drought. In addition, this finding was also consistent with that of Brandt et al. (2018b) who suggested that vegetation productivity decrease associated with the decline of rainfall and soil moisture.

Moreover, water stress was an important limiting factor that controlled terrestrial NPP (Mu et al., 2008), and large-scale droughts have reduced regional NPP globally from 1982 to 1999 (Zhao et al., 2006). The recovery of karst vegetation productivity in the majority of northern provinces mainly benefit from increased P (Fig. 7a, b). This study found that NPP increasing benefited from the contribution of CC controlled by increased P in the majority of karst areas of northwestern China (Fig. S3a), which agreed well with the findings of Zhou et al. (2014) that CC changed from warm-dry to warm-wet in northwestern China (Shi et al., 2007). However, vegetation productivity surprisingly increased remarkably under the scenario of reduced rainfall in some karst areas of the Qinghai-Tibet Plateau. This result was mainly attributed to the rapid growth in SR, which promoted the photosynthesis rate and carbon absorption efficiency in plants growth (Liu et al., 2018; X. Liu et al., 2019; Y. Liu et al., 2019). The increased SR sufficiently offset the restrictions on NPP increasing caused by reduced P. As shown in Fig. S4, the second-order partial correlation between NPP and SR by eliminating the impact of P and T in southern karst areas was higher than that in other karst areas. Moreover, T and P showed high positive correlation with NPP mainly in the areas over 26° N, which also exhibited that SR was the main driving factor for NPP decreasing there. Although the high correlation between NPP and T was shown in VCK area, lower T remained as the main limiting factor for vegetation growth (S. Zhou et al., 2017; W. Zhou et al., 2017), thus contributing less. In addition, the vegetation in karst areas of the Qinghai-Tibet Plateau was mainly covered by grassland with very low productivity (< 100 g C m^{-2} yr^{-1}) (Yan et al., 2019). So, the hydrothermal conditions were not as strict as those in southern karst area with high NPP values (> 500 g C m^{-2} yr^{-1}). Despite the decrease in P, the increased T and SR prolonged the vegetation growth season in the region. Therefore, grassland productivity there exhibited a slower increasing trend. These results were consistent with the result of Li et al. (2016) who demonstrated CC was the dominant factor for mitigation of desertification through accelerating NPP increase there. At the same period, recent climate-induced carbon losses was revealed in African drylands associated with water restriction through satellite passive microwaves (Brandt et al., 2018a), which stressed the importance of water for NPP increasing.

Overall, CC was the dominant factor for vegetation NPP increasing in northern karst areas and controlled the downward trend of vegetation NPP in most southern karst areas. This study also indicated that both T and P obtained the largest negative contributions to NPP variations in TB among all provinces (Fig. 7c,d). As regards the contribution of T in this study was consistent with previous result that the effect of T on NPP variations was very small (Piao et al., 2017; Wang et al., 2003; Yan et al., 2019).

6.4. Effect of endogenous respiration on vegetation productivity

It was observed that the decreased area of GPP was significantly larger than that of autotrophic respiration (Ra), and Ra in many areas where GPP decreased showed an increasing trend (Fig. S5), which indicated that the organic matter accumulated by vegetation through photosynthesis might be consumed by respiration. Previous researches suggested that the increased T and P significantly

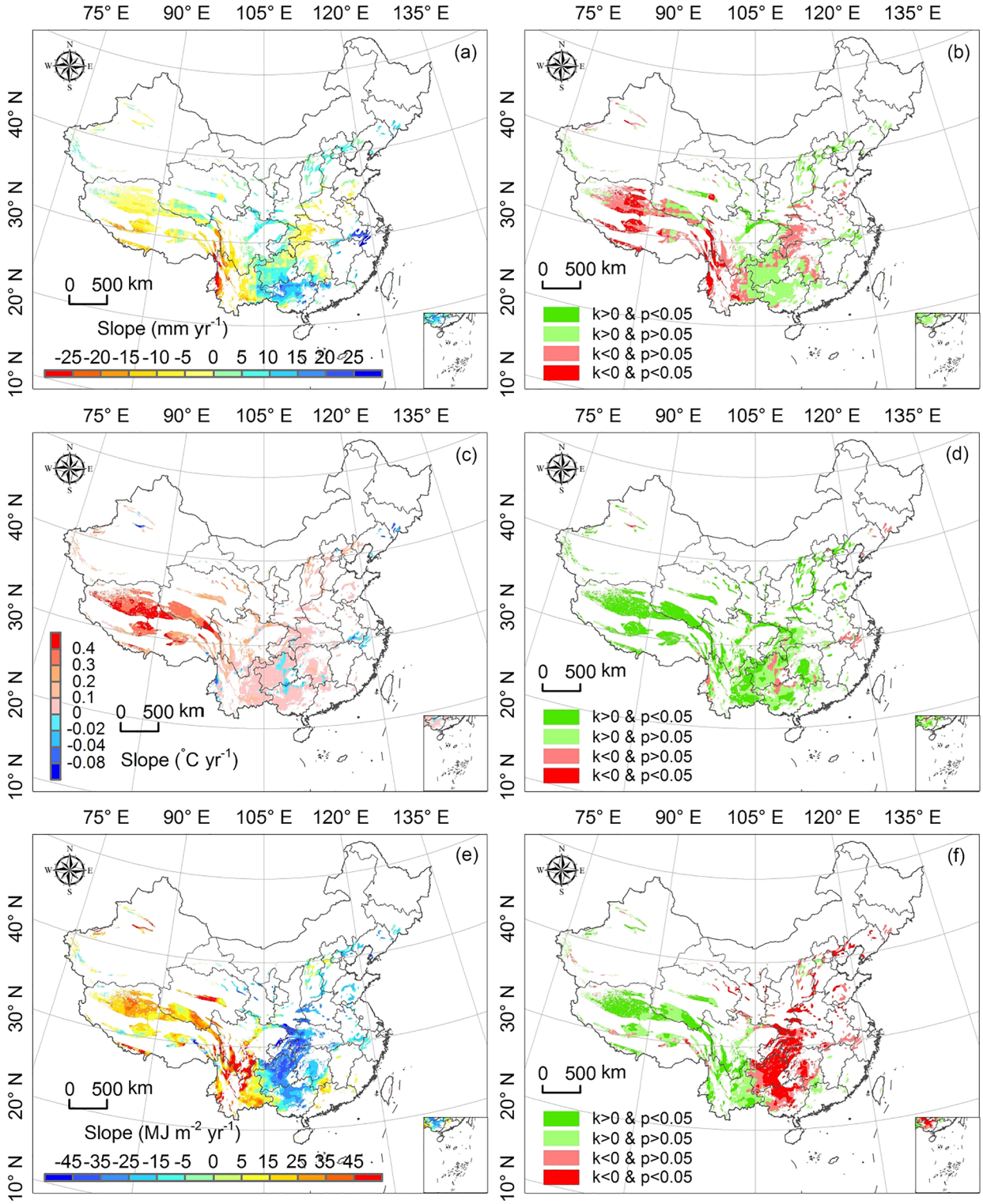

Fig. 7. Variation trends and the significance levels for T (a, b), P (c, d), and SR (e, f) based on spatial pixel. The k in (b, d, and f) represent the slope in (a, c, and e), respectively.

accelerated vegetation Ra (Ryan et al., 1995; Piao et al., 2010; Ben et al., 2018), and promoted the GPP consumption (Ogle, 2018), then reduced NPP storage in vegetation ecosystems, especially in the warm and rainy southern karst area where the growth rate of Ra was much higher than that of carbon sequestration through photosynthesis. Conversely, vegetation required relatively less energy to support metabolism in colder areas of the Qinghai-Tibet Plateau where GPP increasing dominated NPP increasing, resulting in relatively lower Ra consumption (Peng et al., 2017). In southern karst area, photosynthesis was limited by SR, but endogenous Ra increased remarkably due to the significant impact of T and P, which might greatly reduce the net NPP storage. As shown in Fig. 8, 93.41% of NPP growth regions was attributed to the result of GPP accumulation more quickly than Ra consumption. Only 6.59% of that areas was controlled by Ra, which was

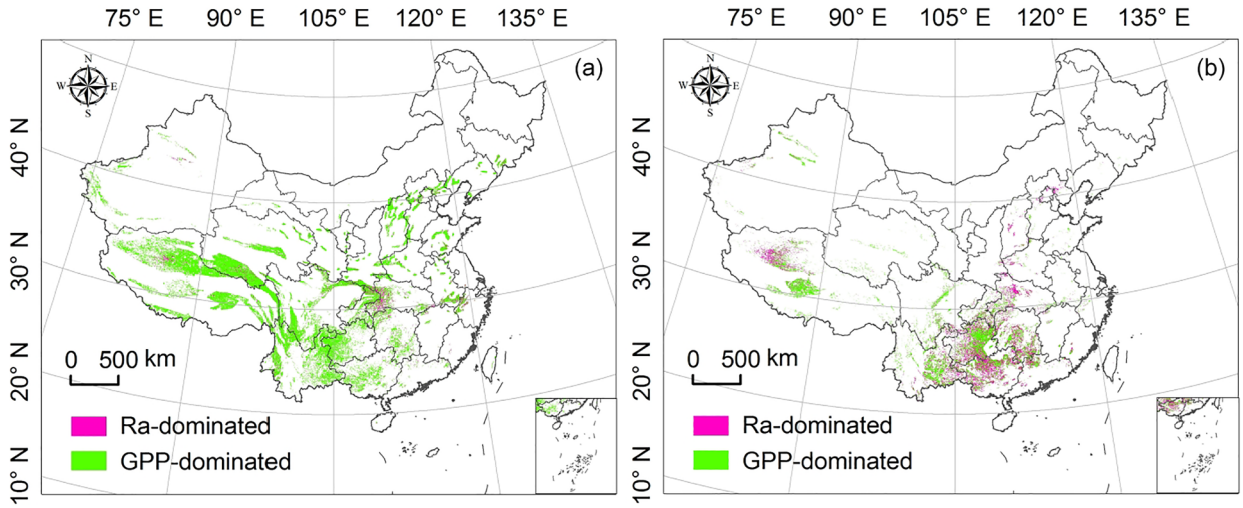

Fig. 8. The GPP- and Ra-dominated NPP increasing zones (a) and decreasing zones (b) in space.

mainly because the decrease rate of Ra was greater than the increase rate of GPP. However, 39.83% of the areas involved in NPP decreasing was attributed to the accelerating consumption of Ra and the rest (60.17%) was contributed by the rapid decrease of GPP.

6.5. Effect of HA on vegetation productivity

Compared with CC, HA was an external driving factor affecting the change of vegetation productivity (Pan et al., 2015). Positive human activities could quickly restore vegetation through ecological engineering and then promoted carbon capture (Tong et al., 2018), whereas negative HA could reduce vegetation rapidly through deforestation and then accelerated carbon release. HA, such as reclamation and deforestation, slash-and-burn cultivation, excessive felling of forests, and overexploitation of water resources, would lead to NPP decreasing, which in turn released more carbon (Jiang et al., 2014; Li et al., 2018a; S. Zhou et al., 2017; W. Zhou et al., 2017). Previous studies showed that HA was an important role in NPP variations by changing the land use structures (Piao et al., 2009). In this study, HA was the major factor in NPP decreasing only in northern GD and eastern YN, and in most northern provinces where the contribution proportions of NPP increasing dominated by HA were less than that dominated by CC. By contrast, HA was the main reason for the reduction in NPP there. This result was consistent with the finding of Zhou et al. (2014) in northwestern China. A similar situation was also observed in sub-Saharan Africa where human population growth offset the climate-driven increase in woody vegetation (Brandt et al., 2017).

But, HA, such as closing mountains for forestry and conversion of farmland to forestry, also promoted the disappearance of rocky desertification and increased vegetation cover and carbon stock (Brandt et al., 2018b; Zhang et al., 2014, 2018). Previous studies suggested that afforestation contributed 25.5% to the greening of vegetation in China (Xiao et al., 2015). The afforestation speed in karst areas had remarkably increased since the launch of the GTGP which was a nationwide ecological project and was started in 2000 in GZ, and continued in GX and YN in 2001. The GTGP was expanded from the original 27 key counties to all counties in three provinces (GZ, GX, and YN) in the following years and a number of conservation projects were implemented in karst areas between 534 m and 1378 m. Large scale afforestation had been carried out involved 325 counties with the conservation areas of 33,094 km^2 during the period 2000–2010 (Tong et al., 2018). 37 counties showed high conservation effort with an average areas of 264 km^2, 96 counties showed moderate conservation effort with an average areas of 141 km^2, 104 counties showed low conservation effort with an average areas of 76 km^2, and only 58 counties showed very low conservation effort with an average areas of 32 km^2 (Tong et al., 2018). In this period, a large area of slope farmland has been converted back to forests and grasslands via ecological projects, which was crucial in promoting NPP increasing in karst areas. We found that the recovery rate of NPP was the fastest at the junction of YN, SC and GZ (Fig. 2c) where HA was the main factor that controlled NPP increasing, which was consistent with the conclusions of Zhou et al. (2017a) and directly corroborated the results of Brandt et al. (2018b) and Tong et al. (2018). Moreover, the influences of HA to NPP variations were positive in southern karst area (i.e., QH, TB, HUB, SC, GZ, GX, HUN, and CQ), which also showed no obvious difference with that from Tong et al. (2018) who demonstrated that HA was the key driving forces for carbon stock through ecological protection measures. Furthermore, the latest study had found a large increase in carbon sequestration of which about half was caused by newly planted and managed forests in southern karst area (Tong et al., 2020). This view also indirectly supported our conclusion that HA contributed positively to vegetation restoration.

Large-scale conservation and ecological projects could contribute to an increasing NPP with positive impacts on carbon storage in karst area. At a small scale, such ecological engineering effects could offset the probabilities of NPP decreasing caused by CC in rocky desertification areas by increasing the vegetation cover. Fortunately, as shown in Fig. 4, CC contributed positively in the regions where ecological projects were implemented by government, such as northwest of GZ, GX, and the border areas of CQ, HUN, and HUB. The low conservation efforts were implemented on a relatively small scale in eastern GZ and northern GX where CC contributed negatively in this study, which was also consistent with the result of Tong et al. (2017) and Tong et al. (2018). These results showed that the conservation projects implemented in these areas were very scientific and reasonable. Unfortunately, the areas where HA continuously showed negative contributions and CC showed weaker positive contributions for NPP increasing were also observed in eastern YN and northern GD. But, some positive changes had also been found in many areas where the total NPP storage reduced due to CC but was compensated by effective ecological projects, which concluded that the positive contribution of HA to NPP increasing could offset the negative contribution of CC. Thus, a large number of ecological projects to promote the restoration of vegetation productivity should be combined with the effects of CC in karst areas of southern China.

Finally, previous studies had shown that China was turning green, and karst vegetation growth made a great contribution to the overall greening (Brandt et al., 2018a; Chen et al., 2002; Yang et al., 2019). Following the start of the GTGP in 2000, the vegetation cover rapidly

increased (+7%) over the karst areas from 1999 to 2012 (Brandt et al., 2018a) and ~5% of the areas with a significant positive biomass trend cover globally were located in southern karst area. However, we had found that vegetation greening (NDVI growth) did not indicate the increase in vegetation productivity. On the contrary, there was also a large area with NPP increasing in the areas where NDVI was decreasing. The possible reason for this inconsistency was that these area might had grown native vegetation and undergone the process of deforestation and reforestation. This was because people had to cultivate a lot of sloping land for cultivation in the early stage of GTGP due to the higher population density in karst area which was much higher than that in non karst area. The areas where deforested first and then reforested would turn green quickly and showed NDVI growth. However, the accumulation process of NPP needed a long time, and it was strongly consumed by respiration, which might lead to the decrease of NPP in some areas.

6.6. Uncertainty and limitation

This study effectively separated and quantitatively assessed the impacts of CC and HA on vegetation productivity in karst area based on partial derivative method, and promoted the deep understanding of the mechanisms of vegetation carbon accumulation. However, we noted that some uncertainties and limitations still remained in our study. Uncertainties in the present study were primarily related to the spatial resolution of the data sets. The resolution of 1 km of the MODIS17A3 data represented mixtures of different vegetation changes, since neither NPP increasing nor decreasing usually covered the full extent of a grid cell. Frequent changes between forestation and vegetation degradation at small scales posed challenges for accurate identification. Although the data source used in this paper was the latest version of MODIS data, it was still the indirect remote sensing data simulated by the model. The main reason was that the measured data in most alpine areas was difficult to obtain. In addition, there were fewer meteorological stations in the Qinghai-Tibet Plateau where karst area was widely distributed, so the widely used and accepted GLDAS 2.1 dataset was used in this study. Moreover, the response of vegetation to CC often showed a lagging effect, which might influence the NPP storage. However, this study failed to consider the lagging effect of NPP caused by meteorological limiting factors. Furthermore, the contributions of CC and HA to NPP changes on multi-time scale were not taken into account in this paper. Due to data limitation, this study had also not further studied the impact of different human management measures on vegetation restoration and its effect identification. These uncertainties and limitations might affect the comprehensiveness of understanding the driving mechanism of vegetation restoration.

6.7. Prospects for future research

This study revealed the key driving factors of ecological restoration and quantified the contribution of these factors to vegetation restoration, and also identified their key control areas. Based on the current research progress, the next study should reveal the differences of contribution values caused by CC and HA between in karst region and non-karst region, especially in the same province. In the future, the main works should focus on the impact of different human management measures on the vegetation ecosystem and its multiscale effect identification on the regional scale on the basis of the preliminary 'Greenization' in the southwest karst area in the early stage, and quantify the carbon sequestration effect and its difference generated by different restoration management measures, especially the carbon water process and its ecological service effect of the plantation restoration. In addition, we should put forward some ideas on how to effectively balance the impact of different restoration management measures on vegetation restoration capacity, such as natural recovery, afforestation, closure and protection. Moreover, we should also attach great importance to the response mechanism of vegetation restoration to drought and extreme climate change, and clarify whether soil moisture will limit the sustainable recovery and growth of forests, so as to prevent the failure of our effort in afforestation over the years. Due to extremely strong human interference, the most important task is to reveal the mutual feeding mechanism between ecological and social systems in the southwest karst region as soon as possible.

7. Conclusions

In this study, the impacts caused by CC and HA on vegetation productivity in karst areas of China were assessed based on partial derivatives to clarify the effect of ecological engineering associated with CC. Then, the contribution proportions of both to NPP increasing and decreasing were further evaluated by setting up eight different scenarios, respectively. The conclusions are as follows:

1) The average NPP over the entire VCK area exhibited an unremarkable increasing trend (0.92 g C m^{-2} yr^{-1}) from 2000 to 2015 and a major decline in NPP was detected in the areas where NDVI increased (0.44 million km^2, 29.07%).
2) Solar radiation (−0.91 g C m^{-2} yr^{-1}) was the preponderant climatic factors exhibiting negative contribution to NPP change.
3) A significant positive contribution was caused by HA (1.53 g C m^{-2} yr^{-1}) on NPP variations, while a negative contribution was induced by CC (−0.61 g C m^{-2} yr^{-1}). For contribution proportions, CC and HA showed the more similar contribution proportion to NPP increasing (51.94% vs 48.06%), but with great difference (68.43% vs 31.57%) for NPP decreasing.
4) 39.83% of the areas involved in NPP decreasing was attributed to the accelerating consumption of Ra and the rest (60.17%) was contributed by the rapid decrease of GPP. But, 93.41% of NPP growth regions was attributed to the result of GPP accumulation more quickly than Ra consumption.
5) In southern karst area, HA showed a positive impact (59.07%) on NPP increasing. However, the negative contribution from CC (70.72%) due to the rapid and constant decline of solar radiation completely counteracted this, leading to a greater NPP decrease.

This study identified the critical control areas in which CC and HA contributed to NPP increasing or decreasing, and suggested that CC weakened the positive effect of ecological engineering on vegetation productivity in southern karst areas. Such insights stressed the importance of negative effect from CC on karst vegetation productivity change and provided location guidance for further implementation of ecological protection projects in southern China. In the future, ecological engineering measures and spatial differences of climate effects should be considered together in karst areas of southern China.

Declaration of Competing Interest

The authors declare that they have no known competing financial interests or personal relationships that could have appeared to influence the work reported in this paper.

Acknowledgements

The National Key Research Program of China (No. 2016YFC0502300 & No. 2016YFC0502102) are supported by the Ministry of Science and Technology, China. Strategic Priority Research Program of the Chinese Academy of Sciences (No. XDA23060100), Western Light Talent Program (Category A) (No. 2018–99), United fund of Karst Science Research Center (No. U1612441) are supported by the

Chinese Academy of Sciences, China. Science and Technology Plan of Guizhou Province of China (No. 2017–2966) is supported by the Department of Science and Technology of Guizhou Province.

Appendix A. Supplementary data

Supplementary data to this article can be found online at https://doi.org/10.1016/j.ecolind.2020.106392.

References

Adams, B., White, A., Lenton, T.M., 2004. An analysis of some diverse approaches to modelling terrestrial net primary productivity. Ecol. Modell. 177, 353–391.

Bai, X.Y., Wang, S.J., Xiong, K.N., 2013. Assessing spatial-temporal evolution processes of karst rocky desertification land: indications for restoration strategies. Land Degrad. Dev. 24 (1), 47–56.

Ben, B.L., Bailey, V.L., Min, C., Gough, C.M., Rodrigo, V., 2018. Globally rising soil heterotrophic respiration over recent decades. Nature 560 (7716), 80–83.

Bjorkman, A.D., Myers-Smith, I.H., Elmendorf, S.C., Normand, S., Rüger, N., Beck, P.S.A., 2018. Plant functional trait change across a warming tundra biome. Nature 562, 57–62.

Brandt, M., Yue, Y., Wigneron, J.P., Tong, X., Tian, F., Jepsen, M.R., 2018b. Satellite-observed major greening and biomass increase in South China karst during recent decade. Earth's Future 6, 1017–1028.

Braswell, B.H., 1997. The response of global terrestrial ecosystems to interannual temperature variability. Science 278 (5339), 870–873.

Brandt, M., Rasmussen, K., Peñuelas, J., Tian, F., Schurgers, G., Verger, A., 2017. Human population growth offsets climate-driven increase in woody vegetation in sub-Saharan Africa. Nat. Ecol. Evol. 1 (4), 0081.

Brandt, M., Wigneron, J.P., Chave, J., Tagesson, T., Penuelas, J., Ciais, P., 2018a. Satellite passive microwaves reveal recent climate-induced carbon losses in African drylands. Nat. Ecol. Evol. 2 (5), 827–835.

Chen, C., Park, T.J., Wang, X.H., Piao, S.L., Xu, B.D., Chaturvedi, R.K., 2019a. China and India lead in greening of the world through land-use management. Nat. Sustain. 122–129.

Chen, W., Chen, J.M., Price, D.T., Cihlar, J., 2002. Effects of stand age on net primary productivity of boreal black spruce forests in ontario, canada. Can. J. Forest Res. 32 (5), 833–842.

Chen, F., Wang, S.J., Bai, X.Y., Liu, F., Zhou, D.Q., Tian, Y.C., et al., 2019b. Assessing spatial-temporal evolution processes and driving forces of karst rocky desertification. Geocarto Int. 1–22.

Delang, C.O., Yuan, Z., 2015. In: China's Grain for Green Program. Springer International Publishing. https://doi.org/10.1007/978-3-319-11505-4.

Donohue, R.J., Roderick, M.L., McVicar, T.R., Farquhar, G.D., 2013. Impact of CO_2 fertilization on maximum foliage cover across the globe's warm, arid environments. Geophys. Res. Lett. 40, 3031–3035.

Fang, J., Guo, Z., Hu, H., Kato, T., Muraoka, H., Son, Y., 2014. Forest biomass carbon sinks in east asia, with special reference to the relative contributions of forest expansion and forest growth. Global Change Biol. 20 (6), 2019–2030.

Fensholt, R., Langanke, T., Rasmussen, K., Reenberg, A., Prince, S.D., Tucker, C., 2012. Greenness in semi-arid areas across the globe 1981–2007 — an earth observing satellite based analysis of trends and drivers. Remote Sens. Environ. 121 (none).

Forkel, M., Carvalhais, N., Schaphoff, S., Von Bloh, W., Thurner, M., Thonicke, K., 2014. Assessing environmental drivers of vegetation greenness by integrating multiple earth observation data in the lpjml dynamic global vegetation model. Genomics 104 (4), 279–286.

Gahlot, S., Shu, S., Jain, A.K., Roy, S.B., 2017. Estimating trends and variation of net biome productivity in india for 1980–2012 using a land surface model. Geophys. Res. Lett. 44, 11573–11579. https://doi.org/10.1002/2017GL075777.

Gollnow, F., Lakes, T., 2014. Policy change, land use, and agriculture: the case of soy production and cattle ranching in Brazil, 2001–2012. Appl. Geogr. 55, 203–211.

Gonsamo, A., Chen, J.M., Lombardozzi, D., 2016. Global vegetation productivity response to climatic oscillations during the satellite era. Global Change Biol.

Guo, Q., Hu, Z., Li, S., Li, X., Sun, X., Yu, G., 2012. Spatial variations in aboveground net primary productivity along a climate gradient in Eurasian temperate grassland: effects of mean annual P and its seasonal distribution. Global Change Biol. 18, 3624–3631.

Haberl, H., Erb, K.H., Krausmann, F., Gaube, V., Bondeau, A., Plutzar, C., Gingrich, S., Lucht, W., Fischer-Kowalski, M., 2007. Quantifying and mapping the humanappropriation of net primary production in earth's terrestrial ecosystems. Proc. Natl. Acad. Sci. U.S.A. 104, 12942–12945.

Hansen, M.C., Potapov, P.V., Moore, R., Hancher, M., Turubanova, S.A., Tyukavina, A., 2013. High-resolution global maps of 21st-century forest cover change. Science 342 (6160), 850–853.

Hasenauer, H., Petritsch, R., Zhao, M., Boisvenue, C., Running, S.W., 2012. Reconciling satellite with ground data to estimate forest productivity at national scales. Forest Ecol. Manage. 276, 196–208.

He, Y., Piao, S., Li, X., Chen, A., Qin, D., 2018. Global patterns of vegetation carbon use efficiency and their climate drivers deduced from modis satellite data and process-based models. Agric. Forest Meteorol. 256–257, 150–158.

Heinsch, F.A., Zhao, M.S., Running, S.W., Kimball, J.S., Nemani, R.R., Davis, K.J., et al., 2006. Evaluation of remote sensing based terrestrial productivity from MODIS using regional tower eddy flux network observations. IEEE Trans. Geosci. Remote Sens. 44 (7), 1908–1925.

Herrmann, S.M., Anyamba, A., Tucker, C.J., 2005. Recent trends in vegetation dynamics in the African Sahel and their relationship to climate. Glob. Environ. Change. 15 (4), 394–404.

Huang, K., Xia, J.Y., Wang, Y.P., Ahlström, A., Chen, J.Q., Cook, R.B., et al., 2018. Enhanced peak growth of global vegetation and its key mechanisms. Nat. Ecol. Evol. 2, 1897–1905.

Jiang, L., Bao, A., Guo, H., Ndayisaba, F., 2017. Vegetation dynamics and responses to climate change and human activities in Central Asia. Sci. Total. Environ. 599, 967–980.

Jiang, Z., Lian, Y., Qin, X., 2014. Rocky desertification insouthwest China: impacts, causes, and restoration. Earth-Sci. Rev. 132, 1–12.

Kato, H., Rodell, M., Beyrich, F., Cleugh, H., van Gorsel, E., Liu, H., Meyers, T.P., 2007. Sensitivity of land surface simulations to model physics, land characteristics, and forcings, at four CEOP sites. J. Meteorol. Soc. JPN 85A, 187–204.

Krausmann, F., Haberl, H., Erb, K., Wiesinger, M., Gaube, V., Gingrich, S., 2009. What determines geographical patterns of the global human appropriation of net primary production? J. Land Use Sci. 4, 15–33.

Li, H.W., Wang, S.J., Bai, X.Y., Luo, W.J., Tang, H., Cao, Y., Wu, L.H., et al., 2018b. Spatiotemporal distribution and national measurement of the global carbonate carbon sink. Sci. Total Environ. 643, 157–170.

Li, J., Wang, Z., Lai, C., Wu, X., Zeng, Z., Chen, X., et al., 2018a. Response of net primary production to land use and land cover change in mainland china since the late 1980s. Sci. Total Environ. 639, 237–247.

Li, Q., Zhang, C., Shen, Y., Jia, W., Li, J., 2016. Quantitative assessment of the relative roles of climate change and human activities in desertification processes on the qinghai-tibet plateau based on net primary productivity. Catena 147, 789–796.

Li, D.K., Wang, Z., 2018. The characteristics of NPP of terrestrial vegetation in China based on MOD17A3 data. Ecol. Environ. Sci. 27 (3), 397–405.

Li, Y.L., Pan, X.Z., Wang, C.K., Liu, Y., Zhao, Q.G., 2014. Changes of vegetation net primary productivity and its driving factors from 2000 to 2011 in Guangxi, China. Acta Ecol. Sin. 34 (18), 5220–5228.

Liu, X., Pei, F., Wen, Y., Li, X., Wang, S., Wu, C., Cai, Y., Wu, J., Chen, J., Feng, K., et al., 2019a. Global urban expansion offsets climate-driven increases in terrestrial net primary productivity. Nat. Clim. Change 10, 5558. https://doi.org/10.1038/s41467-019-13462-1.

Liu, W., Sun, F., 2016. Assessing estimates of evaporative demand in climate models using observed pan evaporation over China. J. Geophys. Res. Atmos. 121 (14), 8329–8349.

Liu, X., Hu, G., Chen, Y., Li, X., Xu, X., Li, S., Wang, S., 2018. High-resolution multi-temporal mapping of global urban land using Landsat images based on the Google Earth Engine Platform. Rem. Sens. Environ. 209, 227–239.

Liu, Y.Y., van Dijk, A.I.J.M., de Jeu, R.A.M., Canadell, J.G., McCabe, M.F., Evans, J.P., Wang, G., 2015. Recent reversal in loss of global terrestrial biomass. Nat. Clim. Change 5 (5), 470–474.

Liu, Y., Yang, Y., Wang, Q., Du, X., Li, J., Gang, C., Wang, Z., 2019b. Evaluating the responses of net primary productivity and carbon use efficiency of global grassland to climate variation along an aridity gradient. Sci. Total. Environ. 652, 671–682.

Ma, Y.H., Fan, S.Y., Zhou, L.H., Dong, Z.H., Zhang, K.C., Feng, J.M., 2007. The temporal change of driving factors during the course of land desertification in arid region of North China: the case of Minqin County. Environ. Geol. 51, 999–1008.

Mao, J., Ribes, Aurélien, Yan, B., Shi, X., Thornton, P.E., Séférian, Roland, et al., 2016. Human-induced greening of the northern extratropical land surface. Nat. Clim. Change 6, 959–963.

Mcmurtrie, R.E., Norby, R.J., Medlyn, B.E., Dewar, R.C., Pepper, D.A., Reich, P.B., 2008. Why is plant-growth response to elevated CO_2 amplified when water is limiting, but reduced when nitrogen is limiting? a growth-optimisation hypothesis. Funct. Plant Biol. 35, 521–534.

Millington, J.D.A., Perry, G.L.W., Romero-Calcerrada, R., 2007. Regression techniques for examining land use/cover change: a case study of a Mediterranean landscape. Ecosystems 10, 562–578.

Morisette, J.T., Privette, J.L., Justice, C.O., 2002. A framework for the validation of MODIS land products. Remote Sens. Environ. 83 (1–2), 77–96.

Mu, Q., Zhao, M., Running, S.W., Liu, M., Tian, H., 2008. Contribution of increasing CO_2 and climate change to the carbon cycle in China's ecosystems. J. Geophys. Res. Biogeosci. 113.

Myneni, R.B., Keeling, C.D., Tucker, C.J., Asrar, G., Nemani, R.R., 1997. Increased plant growth in the northern high latitudes from 1981 to 1991. Nature 386, 698–702.

Nemani, R.R., Keeling, C.D., Hashimoto, H., William, M.J., Stephen, C.P., Compton, J.T., Ranga, M.B., Running, S.W., 2003. Climate-driven increases in global terrestrial net primary production from 1982 to 1999. Science 300, 1560–1563.

Nightingale, J., Nickeson, J.E., Justice, C.O., Baret, F., Garrigues, S., Wolfe, R., 2008. Global Validation of EOS Land Products, Lessons Learned and Future Challenges: A MODIS Case Study. 33rd Proc. of the International Symposium on Remote Sensing of Environment, Stresa, Italy.

Ogle, K., 2018. Hyperactive soil microbes might weaken the terrestrial carbon sink. Nature 560 (7716), 32–33.

Pan, S., Tian, H., Dangal, S.R.S., Ouyang, Z., Tao, B., Ren, W., Lu, C., Running, S.W., 2014. Modeling and monitoring terrestrial primary production in a changing global environment: toward a multiscale synthesis of observation and simulation. Adv. Meteorol. 6426, 1–17.

Pan, S., Tian, H., Lu, C., Dangal, S.R.S., Liu, M., 2015. Net primary production of major plant functional types in China: vegetation classification and ecosystem simulation. Acta Ecol. Sin. 35 (2), 28–36.

Pan, Y., Birdsey, R.A., Fang, J., Houghton, R., Kauppi, P.E., Kurz, W.A., 2011. A large and persistent carbon sink in the world's forests. Science 333.

Peng, D., Zhang, B., Wu, C., Huete, A.R., Wu, Y., 2017. Country-level net primary production distribution and response to drought and land cover change. Sci. Total Environ. 574, 65–77.
Piao, S., Mengtian, H., Zhuo, L., Wang, X., Ciais, P., Canadell, J.G., et al., 2018. Lower land-use emissions responsible for increased net land carbon sink during the slow warming period. Nat. Geosci. 11, 739–743.
Piao, S., Luyssaert, S., Ciais, P., Janssens, I.A., Chen, A., Cao, C., 2010. Forest annual carbon cost: a global-scale analysis of autotrophic respiration. Ecology 91 (3), 652–661.
Piao, S., Liu, Z., Wang, T., Peng, S., Tans, P.P., 2017. Weakening temperature control on the interannual variations of spring carbon uptake across northern lands. Nat. Clim. Change 7 (5), 359–363.
Piao, S., Yin, G., Tan, J., Cheng, L., Huang, M., Li, Y., 2015. Detection and attribution of vegetation greening trend in china over the last 30 years. Glob. Change Biol. 21 (4), 1601–1609.
Piao, S.L., Fang, J., Ciais, P., Peylin, P., Huang, Y., Sitch, S., Wang, T., 2009. The carbon balance of terrestrial ecosystems in China. Nature 458, 1009–1013.
Prestele, R., Arneth, A., Bondeau, A., de Noblet-Ducoudré, N., Pugh, T.A.M., Sitch, S., 2017. Current challenges of implementing anthropogenic land-use and land-cover change in models contributing to climate change assessments. Earth Syst. Dynam. 8 (2), 369–386.
Roderick, M.L., Rotstayn, L.D., Farquhar, G.D., Hobbins, M.T., 2007. On the attribution of changing pan evaporation. Geophys. Res. Lett. 34 (17), L17403.
Rodell, M., Houser, P.R., Jambor, U., Gottschalck, J., Mitchell, K., Meng, C.J., et al., 2004. The global land data assimilation system. B. Am. Meteorol. Soc. 85 (3), 381–394.
Running, S., Mu, Q., Zhao, M., 2015. MOD17A3H MODIS/Terra net primary production yearly L4 Global 500 m SIN Grid V006. NASA EOSDIS Land Processes DAAC.
Ryan, M.G., Gower, S.T., Hubbard, R.M., Waring, R.H., Gholz, H.L., Cropper, W.P., 1995. Woody tissue maintenance respiration of four conifers in contrasting climates. Oecologia (Berlin) 101 (2), 133–140.
Schweizer, P.E., Matlack, G.R., 2014. Factors driving land use change and forest distribution on the coastal plain of Mississippi, USA. Landsc. Urban Plan. 121, 55–64.
Shi, Y.F., Shen, Y.P., Kang, E., Li, D.L., Ding, Y.J., Zhang, G.W., Hu, R.J., 2007. Recent and future climate change in northwest China. Clim. Change 80, 379–393.
Smith, B., Wårlind, D., Arneth, A., Hickler, T., Leadley, P., Siltberg, J., 2014. Implications of incorporating n cycling and n limitations on primary production in an individual-based dynamic vegetation model. Biogeosciences 11 (7), 2027–2054.
Tian, H., Melillo, J., Lu, C., Kicklighter, D., Liu, M., Ren, W., 2011. China's terrestrial carbon balance: contributions from multiple global change factors. Global Biogeochem. Cy. 25, GB1007.
Tian, Y.C., Wang, S.J., Bai, X.Y., Luo, G.J., Xu, Y., 2016. Trade-offs among ecosystem services in a typical karst watershed, SW China. Sci. Total Environ. 566–567, 1297–1308.
Tong, X., Brandt, M., Yue, Y., Ciais, P., Rudbeck Jepsen, M., Penuelas, J., et al., 2020. Forest management in southern China generates short term extensive carbon sequestration. Nat. Commun. 11 (1). https://doi.org/10.1038/s41467-019-13798-8.
Tong, X., Brandt, M., Yue, Y., Horion, S., Wang, K., Keersmaecker, W.D., 2018. Increased vegetation growth and carbon stock in china karst via ecological engineering. Nat. Sustain. 1 (1), 44–50.
Tong, X., Wang, K., Yue, Y., Brandt, M., Liu, B., Zhang, C., 2017. Quantifying the effectiveness of ecological restoration projects on long-term vegetation dynamics in the karst regions of southwest china. Int. J. Appl. Earth Obs. Geoinf. 54, 105–113.
Wang, J., Rich, P.M., Price, K.P., 2003. Temporal responses of NDVI to precipitation and temperature in the central Great Plains, USA. Int. J. Remote Sens. 24, 2345–2364.
Wang, Z., Zhang, Y., Yang, Y., Zhou, W., Gang, C., Zhang, Y., Qi, J., 2016. Quantitative assess the driving forces on the grassland degradation in the Qinghai-Tibet Plateau, in China. Ecol. Inform. 33, 32–44.
Wen, Y., Liu, X., Pei, F., Li, X., Du, G., 2018. Non-uniform time-lag effects of terrestrial vegetation responses to asymmetric warming. Agric. For. Meteorol. 252, 130–143.
Wu, D., Zhao, X., Liang, S., Zhou, T., Huang, K., Tang, B., et al., 2015. Time-lag effects of global vegetation responses to climate change. Glob. Change Biol. 21 (9), 3520.
Wu, L., Wang, S., Bai, X., Luo, W., Tian, Y., Zeng, C., Luo, G., He, S., 2017. Quantitative assessment of the impacts of climate change and human activities on runoff change in a typical karst watershed, SW China. Sci. Total Environ 601–602, 1449–1465.
Xiao, J., Zhou, Y., Zhang, L., 2015. Contributions of natural and human factors to increases in vegetation productivity in China. Ecosphere 6 (11), 233.
Xu, C., McDowell, N.G., Fisher, R.A., Wei, L., Sevanto, S., Christoffersen, B.O., Weng, E., Middleton, R.S., 2019. Increasing impacts of extreme droughts on vegetation productivity under climate change. Nat. Clim. Change 9 (12), 948–953 https://doi.org/doi:10.1038/s41558-019-0630-6.
Xu, X.L., 2018. Spatial distribution data set of China's annual vegetation index (NDVI). Data registration and publishing system of resource and environment science data center of Chinese Academy of Sciences (http://www.resdc.cn/DOI).
Xu, D.Y., Kang, X.W., Zhuang, D.F., Pan, J.J., 2010. Multi-scale quantitative assessment of the relative roles of climate change and human activities in desertification-a case study of the Ordos Plateau, China. J. Arid Environ. 74 (4), 498–507.
Yan, Y.C., Liu, X.P., Wen, Y.Y., Ou, J.M., 2019. Quantitative analysis of the contributions of climatic and human factors to grassland productivity in northern China. Ecol. Indic. 103, 542–553.
Yang, Y., Wang, S., Bai, X., Tan, Q., Li, Q., Wu, L., 2019. Factors affecting long-term trends in global NDVI. Forests 10 (5), 372.
Ye, L., Fang, L., Shi, Z., Deng, L., Tan, W., 2019. Spatio-temporal dynamics of soil moisture driven by 'Grain for Green' program on the Loess Plateau, China. Agric. Ecosyst. Environ. 269, 204–214.
You, G., Zhang, Y., Liu, Y., Song, Q., Lu, Z., Tan, Z., Xie, Y., 2013. On the attribution of changing pan evaporation in a nature reserve in SW China. Hydrol. Process. 27 (18), 2676–2682.
Yu, G.R., Zhu, X.J., Fu, Y.L., He, H.L., Wang, Q.F., Wen, X.F., 2013. Spatial patterns and climate drivers of carbon fluxes in terrestrial ecosystems of China. Glob. Change Biol. 19, 798–810.
Zeng, Z.Z., Lyndon, E., Ziegler, A.D., Anping, C., Timothy, S., Fangyuan, H., et al., 2018. Highland cropland expansion and forest loss in Southeast Asia in the twenty-first century. Nat. Geosci. 11, 556.
Zhang, C., Qi, X., Wang, K., Zhang, M., Yue, Y., 2017. The application of geospatial techniques in monitoring karst vegetation recovery in southwest China: a review. Prog. Phys. Geog. 41 (4), 450–477.
Zhang, M., Wang, K., Liu, H., Zhang, C., Yue, Y., Qi, X., 2018. Effect of ecological engineering projects on ecosystem services in a karst region: a case study of northwest Guangxi, China. J. Clean. Prod. 183, 831–842.
Zhang, M.Y., Wang, K.L., Liu, H.Y., Jing, W., Yue, Y.M., 2014. Impacts of ecological restoration on vegetation carbon storage in the typical karst region of northwest Guangxi, China. Chin. J. Ecol. 33 (9), 2288–2295.
Zhang, Y.J., Xu, M., Chen, H., Adams, J., 2009. Global pattern of NPP to GPP ratio derived from MODIS data: effects of ecosystem type, geographical location and climate. Glob. Ecol. Biogeogr. 18 (3), 280–290.
Zhao, M., Heinsch, F.A., Nemani, R.R., Running, S.W., 2005. Improvements of the MODIS terrestrial gross and net primary production global data set. Remote Sens. Environ. 95 (2), 164–176.
Zhao, M., Running, S.W., 2010. Drought-induced reduction in global terrestrial net primary production from 2000 through 2009. Science 329, 940–943.
Zhao, M., Running, S.W., Nemani, R.R., 2006. Sensitivity of Moderate Resolution Imaging Spectroradiometer (MODIS) terrestrial primary production to the accuracy of meteorological reanalyses. J. Geophys. Res. 111, G01002.
Zhou, W., Yang, H., Huang, L., Chen, C., Lin, X., Hu, Z., Li, J., 2017b. Grassland degradation remote sensing monitoring and driving factors quantitative assessment in China from 1982 to 2010. Ecol. Indic. 83, 303–313.
Zhou, W., Gang, C., Zhou, F., Li, J., Dong, X., Zhao, C., 2015. Quantitative assessment of the individual contribution of climate and human factors to desertification in northwest China using net primary productivity as an indicator. Ecol. Indic. 48, 560–569.
Zhou, W., Gang, C., Zhou, L., Chen, Y., Li, J., Ju, W., Odeh, I., 2014. Dynamic of grassland NPP decreasing and its quantitative assessment in the northwest China. Acta Oecol. 55, 86–96.
Zhou, S., Yu, B., Schwalm, C.R., Ciais, P., Zhang, Y., Fisher, J.B., 2017a. Response of water use efficiency to global environmental change based on output from terrestrial biosphere models. Global. Biogeochem. Cy. 31, 1639–1655.
Zhu, W., Pan, Y., Yang, X., Song, G., 2007. Impact of climate change on net primary productivity of China's terrestrial vegetation. Chin. Sci. Bull. 52 (21), 2535–2541.
Zhu, Z., Piao, S., Myneni, R.B., Huang, M., Zeng, N., 2016. Greening of the earth and its drivers. Nat. Clim. Change 6 (8), 791–795.
Zscheischler, J., Reichstein, M., Buttlar, J.V., Mu, M., Mahecha, M.D., 2014. Carbon cycle extremes during the 21st century in CMIP5 models: future evolution and attribution to climatic drivers. Geophys. Res. Lett. 41 (24), 8853–8861.